Numerical Hermitian Yang-Mills Connections and Vector Bundle Stability in Heterotic Theories

Lara B. Anderson[1], Volker Braun[2], Robert L. Karp[3], and Burt A. Ovrut[1]

[1] *Department of Physics, University of Pennsylvania 209 South 33rd Street, Philadelphia, PA 19104-6395, U.S.A.*

[2] *Dublin Institute for Advanced Studies 10 Burlington Road, Dublin 4, Ireland*

[3] *Department of Physics, Virginia Polytechnic Institute and State University, Blacksburg, VA 24061, U.S.A.*

Abstract

A numerical algorithm is presented for explicitly computing the gauge connection on slope-stable holomorphic vector bundles on Calabi-Yau manifolds. To illustrate this algorithm, we calculate the connections on stable monad bundles defined on the $K3$ twofold and Quintic threefold. An error measure is introduced to determine how closely our algorithmic connection approximates a solution to the Hermitian Yang-Mills equations. We then extend our results by investigating the behavior of non slope-stable bundles. In a variety of examples, it is shown that the failure of these bundles to satisfy the Hermitian Yang-Mills equations, including field-strength singularities, can be accurately reproduced numerically. These results make it possible to numerically determine whether or not a vector bundle is slope-stable, thus providing an important new tool in the exploration of heterotic vacua.

Email: andlara@physics.upenn.edu, vbraun@stp.dias.ie, rlk@vt.edu, ovrut@elcapitan.hep.upenn.edu

Contents

1 Introduction

1.1 The Generalized Donaldson Algorithm and Heterotic Compactifications

A central goal of string theory is to produce low-energy theories with the symmetries, spectrum and properties of elementary particle physics. In the search for realistic vacua, compactification of the heterotic string [1, 2] and M-theory [3, 4, 5] on smooth Calabi-Yau threefolds with holomorphic vector bundles [6, 7, 8, 9, 10, 11, 12] has played an important role [13, 14, 15, 16, 17].

Heterotic compactifications possess a number of phenomenologically desirable features, including realistic gauge groups and particle spectra [18, 19, 20, 21, 22, 23, 24, 25] as well as gauge coupling unification [26, 27]. However, certain fundamental quantities, such as the Yukawa couplings, are difficult to compute directly [28, 29, 30, 31, 32, 33]. For example, the "physical" Yukawa couplings depend on both the Yukawa coefficients in the superpotential and the explicit form of the Kähler potential. Both quantities are determined by the detailed structure of the underlying geometry–specifically, the metric on the Calabi-Yau threefold and the connection on the slope-stable holomorphic vector bundle–about which, generically, little is known. It follows that the Yukawa couplings in the four-dimensional effective theory have not been explicitly computed, except in very special cases where sophisticated tools from algebraic geometry or topological string theory are available. As a result, one can rarely do better than the qualitative statement that such coupling coefficents either vanish or are "of order one".

To fully specify the geometry and, hence, to be able to compute the couplings in the effective theory, one must determine the Ricci-flat metric g on the Calabi-Yau threefold X and the supersymmetric gauge connection A on the slope-stable holomorphic vector bundle $\mathcal{V}$ [34]. Yau's theorem [35] gives an existence proof for the Ricci-flat metric and the work of Donaldson-Uhlenbeck-Yau [36, 37] provides us with a class of holomorphic vector bundles, called slope-stable, that are consistent with supersymmetry. However, in general the form of g and A are not known analytically. The technical challenge of determining these quantities has made systematic studies of realistic heterotic vacua difficult to achieve.

In recent years, a number of new numerical approaches to these old problems have been presented [38, 39, 40, 41, 42, 43, 44, 45, 46, 47]. Thanks to the development of powerful new algorithms and increased computer speed, it is now possible to compute Ricci-flat metrics and to directly solve the Hermitian Yang-Mills equations for the gauge connection. With this data in hand, all quantities in the four-dimensional effective theory, such as the correctly normalized zero modes, all coefficients in the superpotentials and the Kähler potential, can, in principle, be computed. In this paper, we take several important new steps towards this goal. The paper is structured as follows.

In Section 2, we outline the general form of Donaldson's algorithm for computing the Ricci-flat metric [38, 39, 40] on a Calabi-Yau manifold. Specifically, using the numerical implementations developed in [48, 49] and [50, 43], we calculate Ricci-flat metrics on the $K3$ surface and the Quintic threefold. To evaluate the accuracy of our approximation scheme, that is, how close our approximate metric is to the Ricci-flat solution, several measures of the metric-error are introduced. In Section 3, we turn our attention to recent generalizations of Donaldson's algorithm due to Yau, Wang and Douglas et. al. [42, 43]. These make it possible to compute Hermitian-Einstein metrics on holomorphic vector bundles over a Calabi-Yau manifold and, hence, to solve for the gauge connection satisfying the conditions for $\mathcal{N} = 1$ supersymmetry.

Given a rank n holomorphic vector bundle $\mathcal{V}$ on a Calabi-Yau manifold X, the central idea of the algorithm rests on establishing an embedding of X into a Grassmanian $G(n, N_k - 1)$ via the N_k sections of $\mathcal{V} \otimes \mathcal{L}^{\otimes k}$, where $\mathcal{L}$ is some ample line bundle. Using this embedding, a family of simple Kähler metrics on $G(n, N_k - 1)$ can be pulled-back to the Calabi-Yau manifold and used to define a sequence of Hermitian fiber metrics converging to a Hermitian-Einstein metric on $\mathcal{V}$. In [42, 50], Wang proposed a generalization of Donaldson's "T-operator" for the embedding described above. It was shown that the iteration of this T-operator converges to a fixed point for each value of k if and only if the bundle $\mathcal{V}$ is Gieseker-stable. Furthermore, in the case that $\mathcal{V}$ is slope-stable, there exists a scheme of approximate fiber metrics on $\mathcal{V}$ which converges to the Hermitian-Einstein metric in the limit that $k \to \infty$. Wang's results are reviewed in Section 3.1. We then *present a new algorithm to explicitly construct the Hermitian-Einstein fiber metric and, hence, the supersymmetric gauge connection A on $\mathcal{V}$*. An interesting technical aspect arises in the process of extracting the connection on $\mathcal{V}$ from the connection produced by the algorithm on the "twisted" bundle $\mathcal{V} \otimes \mathcal{L}^{\otimes k}$. In Section 3.2, by studying all possible methods of "untwisting" the bundle, we establish the computationally optimal choice and present a general procedure for the computation of the connection on $\mathcal{V}$ itself. Following Wang's theorem (Theorem 4 in Section 3.1), we *explicitly compute the connection on several slope-stable vector bundles, beginning in Section 3.3, and develop an accurate error measure, τ_{k_H}, to quantify the accuracy of numerical approximations.*

In Section 4, we move beyond Wang's theorem and explore the behavior of non-stable bundles under the generalized Donaldson algorithm. Since Wang's theorem does not apply in this case, there is, a priori, no reason to expect any specific behavior or systematic results from the algorithm. We show, however, that *the output of Donaldson's algorithm, when applied to properly semi-stable or unstable bundles, can in be understood in terms of their Harder-Narasimhan filtrations. Furthermore, it is shown in detail that the failure of these bundles to satisfy the Hermitian Yang-Mills equations, ranging from non-trivial constants to field-strength singularities, can be accurately reproduced numerically.* These observations demonstrate that Donaldson's algorithm provides an important new tool in the study of the slope-stability properties

of vector bundles. In an arbitrary heterotic compactification, one of the most difficult obstacles to overcome is deciding whether or not a given vector bundle is slope-stable. This determination has hithertofore required analytically determining all subsheaves of the bundle and calculating their slopes. This, at best, is a difficult thing to do, and often cannot be carried out. In this paper, we show that *the stability properties of a vector bundle, that is, whether it is stable, semi-stable or unstable, can always be determined by numerical calculation using the generalized Donaldson's algorithm. This result provides a new tool in the exploration of supersymmetric heterotic vacua. We illustrate these procedures by looking at a variety of stable, semi-stable, and unstable bundles on the $K3$ twofold and the Quintic threefold.* The bundles we choose as examples are defined via the monad construction [51, 52, 53, 25], a class known to contain bundles corresponding to physically realistic heterotic compactifications.

In the following two subections, we set the stage for the entire discussion by defining the Hermitian Yang-Mills equations and their relationship to the slope-stabilty of vector bundles [54].

1.2 The Hermitian Yang-Mills Equations and Hermitian-Einstein Bundle Metrics

An $\mathcal{N} = 1$ supersymmetric heterotic string compactification is specified by a complex three-dimensional Calabi-Yau manifold, X, and a holomorphic vector bundle, $\mathcal{V}$, with structure group $K \subset E_8$ defined over X. The gauge connection, A, on $\mathcal{V}$ with associated field strength, F, must satisfy the well-known equations [34]

$$F_{ij} = F_{\bar{i}\bar{j}} = 0, \quad g^{i\bar{j}} F_{i\bar{j}} = 0 \tag{1.1}$$

where $i, j = 1, 2, 3$ run over the holomorphic indices of the Calabi-Yau threefold. These equations arise as the vanishing condition on the variation of the 10-dimensional gaugino and, hence, are required to preserve $\mathcal{N} = 1$ supersymmetry. The first two conditions, $F_{ij} = F_{\bar{i}\bar{j}} = 0$, are simply the constraint that the vector bundle be holomorphic. On a holomorphic vector bundle, that is, one with holomorphic transition functions, one can always choose a connection with a purely $(1, 1)$ field strength. Hence, the vanishing of the $(2, 0)$ and $(0, 2)$ components is satisfied. The last condition, $g^{i\bar{j}} F_{i\bar{j}} = 0$, however, is not so easily solved. Equations (1.1) are a special case of the Hermitian Yang-Mills equations. More generally, one has

$$g^{i\bar{j}} F_{i\bar{j}} = c \cdot \mathbf{1} \tag{1.2}$$

where c is a constant determined by the first Chern class of the bundle $\mathcal{V}$. For a generic holomorphic, rank n vector bundle, the structure group is realized in the fundamental representation of $U(n)$. Then $c_1(\mathcal{V}) \neq 0$ and, therefore, $c \neq 0$. However, for strucure group $K \subset E_8$, it follows that $c_1(\mathcal{V})$ must vanish; hence, the zero trace in (1.1). The numerical algorithms in this paper will require us to find solutions to the general

equation (1.2). The results will then be specializing to the case $c = 0$, that is, (1.1), relevant for heterotic compactifications.

A solution to (1.2) is equivalent to the bundle $\mathcal{V}$ carrying a particular Hermitian structure. An Hermitian structure (or Hermitian fiber metric), G, on $\mathcal{V}$ is an Hermitian scalar product G_x on each fiber $\mathcal{V}(x)$ which depends differentiably on x. The pair $(\mathcal{V}, G)$ is often referred to as an Hermitian vector bundle. For a given choice of frame, $e_a(x)$, for the bundle, one can define the covariant derivative as

$$D(v^a e_a) = (dv^a)e_a + v^a A^b_a e_b \ , \tag{1.3}$$

where $a, b = 1, \ldots n$ take values in the structure group $K \subset U(n)$. The Hermitian structure defines an inner product as

$$(e_a, e_b) = G_{\bar{a}b}, \quad G = G^\dagger. \tag{1.4}$$

The condition that the connection be compatible with the metric,

$$d(u, v) = (Du, v) + (u, Dv) \ , \tag{1.5}$$

gives

$$\partial G_{\bar{a}b} = G_{\bar{a}c} A^c_b \tag{1.6}$$

and, hence,

$$A = G^{-1}\partial G \ . \tag{1.7}$$

Since one can always make a gauge choice to set $\bar{A} = 0$ for a holomorphic bundle, we can re-phrase the Hermitian Yang-Mills equation (1.2) on $F^{(1,1)}$ as a condition on the metric,

$$c \cdot \mathbf{1} = g^{i\bar{j}} F_{i\bar{j}} = g^{i\bar{j}} \bar{\partial}_{\bar{j}} A_i = g^{\bar{j}i} \bar{\partial}_{\bar{j}} (G^{-1} \partial_i G) \ . \tag{1.8}$$

A metric G on the fiber of V satisfying the above equation is called an Hermitian-Einstein metric.

Finally, note that given a fiber metric G, one can define an inner product on the space of global sections, s^a_α where $\alpha = 1, \ldots h^0(X, \mathcal{V})$, of $\mathcal{V}$ as

$$< s_\alpha | s_\beta >= \int_X \left(s^b_\beta G_{b\bar{a}} \bar{s}^{\bar{a}}_{\bar{\alpha}} \right) dVol \ . \tag{1.9}$$

This will be of use to us in subsequent sections. Before attempting to explicitly construct a connection A on $\mathcal{V}$ satisfying (1.2) (or, equivalently, an Hermitian-Einstein bundle metric satisfying (1.8)), we will first rephrase these conditions in terms of algebraic geometry and recall a central theorem.

1.3 Slope Stability

Having presented the Hermitian Yang-Mills equations and defined Hermitian-Einstein bundle metrics, we now introduce one more important mathematical notion. As stated above, the Hermitian Yang-Mills equation $g^{i\bar{j}}F_{\bar{j}i} = c \cdot \mathbf{1}$ is notoriously difficult to solve for the case of non-Abelian structure groups. However, on Calabi-Yau manifolds there exists a powerful method for transforming this equation into a problem in algebraic geometry. For Kähler manifolds, the Donaldson-Uhlenbeck-Yau theorem [36, 37] states that on each *poly-stable* holomorphic vector bundle $\mathcal{V}$ there exists a unique connection satisfying the Hermitian Yang-Mills equation (1.2). Thus, to verify that a vector bundle is consistent with supersymmetry, one need only verify that it possesses the property of poly-stability.

The notion of slope-stability (also referred to as Mumford-Takemoto stability) of a bundle (or coherent sheaf), $\mathcal{F}$, over a Kähler manifold, X, is defined by means of a real number called the *slope*:

$$\mu(\mathcal{F}) \equiv \frac{1}{\mathrm{rk}(\mathcal{F})} \int_X c_1(\mathcal{F}) \wedge \omega^{d-1}, \tag{1.10}$$

where d is the dimension of the Kähler manifold. Here, ω is the Kähler form on X, while $\mathrm{rk}(\mathcal{F})$ and $c_1(\mathcal{F})$ are the rank and the first Chern class of $\mathcal{F}$ respectively. A bundle $\mathcal{V}$ is called *stable* (*semi-stable*) if for all sub-sheaves $\mathcal{F} \subset \mathcal{V}$ with $0 < \mathrm{rk}(\mathcal{F}) < \mathrm{rk}(\mathcal{V})$ the slope satisfies

$$\mu(\mathcal{F}) < \mu(\mathcal{V}) \qquad (\mu(\mathcal{F}) \leq \mu(\mathcal{V})) \ . \tag{1.11}$$

A bundle is *poly-stable* if it can be decomposed into a direct sum of stable bundles which all have the same slope. That is,

$$\mathcal{V} = \bigoplus_n \mathcal{V}_n \ , \qquad \mu(\mathcal{V}_i) = \mu(\mathcal{V}) \ . \tag{1.12}$$

Thus, stability is a special case of poly-stability which is in turn a subset of semi-stability. As a series of implications: stable $\Rightarrow$ poly-stable $\Rightarrow$ semi-stable. It is important to note that the converse to these statements do not hold. For example, not every semi-stable bundle is poly-stable. Finally, observe that the slope is exactly the constant, c, that appeared in (1.2). Written in terms of the slope of $\mathcal{V}$, the general Hermitian Yang-Mills condition is

$$g^{i\bar{j}}F_{i\bar{j}} = \mu(\mathcal{V}) \cdot \mathbf{1}_{n\times n} \ , \tag{1.13}$$

where n is the rank of $\mathcal{V}$ and $\mu(\mathcal{V})$ is defined in (1.10).

It should be noted that the condition of slope-stability on a Calabi-Yau manifold depends on all moduli of the heterotic compactification. To be specific, consider a Calabi-Yau threefold. Here, the moduli are the Kähler moduli ($h^{1,1}(X)$), the complex structure moduli ($h^{2,1}(X)$) and the vector bundle moduli ($h^1(End(\mathcal{V}))$). The

dependence on Kähler moduli is explicit in (1.1) and referred to as a choice of "polarization". One can expand the Kähler form ω in (1.10) as $\omega = t^r\omega_r$, where ω_r form a basis of $(1,1)$-forms and t^r are the real parts of the Kähler moduli. Written in terms of the triple intersection numbers, d_{rst}, of the threefold, the slope is simply $\mu(\mathcal{V}) = \frac{1}{rk(\mathcal{V})} d_{rst} c_1(\mathcal{V})^r t^s t^t$ where $r, s = 1, \ldots h^{1,1}(X)$. The other moduli enter through the notion of a subsheaf $\mathcal{F} \in \mathcal{V}$. In general, whether or not there exists an injective sheaf morphism $\phi : \mathcal{F} \to \mathcal{V}$ depends on both the complex structure moduli and the vector bundle moduli.

Thus, finding a solution to the Hermitian Yang-Mills equations (that is, determining whether the bundle is slope-stable) is a question that must be asked after selecting a particular point in moduli space. As we will see, some regions of moduli space may admit a solution while others will not. This moduli dependence can lead to a variety of interesting physical consequences [55, 56, 57, 58], which we will explore in later sections. For most of this work, however, we will be interested in studying the stability properties of bundles at "generic" points in their moduli space.

Before investigating solutions to the Hermitian Yang-Mills equations, we must first introduce an algorithmic approach to determining Hermitian metrics (both of manifolds and bundles). In the following section, we discuss Donaldson's algorithm for numerically approximating the Ricci-flat metric on a Calabi-Yau manifold.

2 Computing the Calabi-Yau Metric

2.1 Donaldson's Algorithm

Many of the challenges associated with string compactifications on a Calabi-Yau threefold, X, arise from the difficulty in determining the explicit geometry. The simplest $\mathcal{N} = 1$ supersymmetric vacuum solutions require a Ricci-flat metric, $g_{i\bar{j}}$, on X. While Yau's theorem [35] ensures that such a metric exists, no analytic solutions have been found. Recently, however, it has become possible to find numerical solutions using an algorithm developed by Donaldson [38, 39, 40]. This algorithm has been implemented numerically and extended in [59, 48, 49, 50, 43, 46]. For other numerical computations of Kähler metrics, see [44, 60, 45]. In this paper, we propose to investigate solutions to the Hermitian Yang-Mills equation $g^{i\bar{j}} F_{i\bar{j}} = 0$. Since the Ricci-flat metric, $g_{i\bar{j}}$, is required for such a solution, in this section we provide a brief review of Donaldson's algorithm for approximating such metrics on Calabi-Yau manifolds.

The starting point of Donaldson's algorithm is the observation that there exists a natural metric on $\mathbb{P}^n$. Denoting the $n+1$ homogeneous coordinates by z_i, this Fubini-Study metric is given by $g_{FSi\bar{j}} = \frac{i}{2}\partial_i \bar{\partial}_{\bar{j}} K_{FS}$, where

$$K_{FS} = \frac{1}{\pi} \ln \sum_{i\bar{j}} h^{i\bar{j}} z_i \bar{z}_{\bar{j}} \tag{2.1}$$

and $h^{i\bar{j}}$ is any hermitian, non-singular matrix. The Fubini-Study metric is usually defined with $h^{i\bar{j}} = \delta^{i\bar{j}}$, but we will refer to (2.1) as a Fubini-Study Kähler potential for any hermitian matrix $h^{i\bar{j}}$. The Fubini-Study metric can be used to induce a metric on any subvariety of $\mathbb{P}^n$. In particular, it will induce a metric on any Calabi-Yau threefold X, since it is always possible to embed $X \subset \mathbb{P}^n$ for some n. However, such a metric will not, in general, be Ricci-flat. To obtain the Ricci-flat metric, Donaldson's algorithm requires one to use a generalized version of (2.1) with enough free parameters to provide a more versatile induced metric on X. The algorithm then guarantees that this generalized metric will converge, in some specified limit, to the Ricci-flat metric.

An obvious generalization of (2.1) is to replace the degree one polynomials with polynomials of higher degree. For example,

$$K = \frac{1}{k\pi} \ln \sum_{i_1 \ldots i_k \bar{j}_1 \ldots \bar{j}_k} h^{i_1 \ldots i_k \bar{j}_1 \ldots \bar{j}_k} z_{i_1} \ldots z_{i_k} \bar{z}_{\bar{j}_1} \ldots \bar{z}_{\bar{j}_k} \tag{2.2}$$

where $h^{i_1 \ldots i_k \bar{j}_1 \ldots \bar{j}_k}$ is hermitian. This new Kähler potential now has $(n+1)^{2k}$ real parameters. One can write the above generalization in a more systematic way by noting that such Kähler potentials can naturally be obtained by considering holomorphic line bundles on the Calabi-Yau manifold X itself and using the Kodaira embedding theorem. Let $\mathcal{L}$ be a holomorphic line bundle over X with $n_1 = h^0(X, \mathcal{L})$ global sections. Consider a twisting of the line bundle, $\mathcal{L}^k = \mathcal{L}^{\otimes k}$. Then, choosing a basis for the space of sections, $s_\alpha \in H^0(X, \mathcal{L}^k)$ where $0 \leq \alpha \leq n_k - 1$, allows one to define a map from X to $\mathbb{P}^{n_k - 1}$ given by

$$i_k : \; X \to \mathbb{P}^{n_k - 1}, \quad (x_0, \ldots, x_2) \mapsto \left[s_0(x) : \ldots : s_{n_k - 1}(x) \right] \; , \tag{2.3}$$

where x_i are holomorphic coordinates on the Calabi-Yau threefold. The Kodaira embedding theorem [61] states that if $\mathcal{L}$ is ample, (2.3) will define an embedding of $X \subset \mathbb{P}^{n_k - 1}$ for all $\mathcal{L}^k$ with $k \geq k_0$ for some k_0.

In terms of this natural embedding line bundle, we can view the generalized Kähler potential (2.2) restricted to X simply as

$$K_{h,k} = \frac{1}{k\pi} \ln \sum_{\alpha, \bar{\beta} = 0}^{n_k - 1} h^{\alpha \bar{\beta}} s_\alpha \bar{s}_{\bar{\beta}} = \ln ||s||^2_{h,k} \; . \tag{2.4}$$

Geometrically, (2.4) defines an hermitian metric on the line bundle $\mathcal{L}^k$ itself. It provides a natural inner product on the space of global sections

$$M_{\alpha \bar{\beta}} = \langle s_\beta | s_\alpha \rangle = \frac{n_k}{\mathrm{Vol}_{CY}(X)} \int_X \frac{s_\alpha \bar{s}_{\bar{\beta}}}{||s||^2_h} \, \mathrm{dVol}_{CY} \; , \tag{2.5}$$

where

$$\mathrm{dVol}_{\mathrm{CY}} = \Omega \wedge \bar{\Omega} \tag{2.6}$$

and Ω is the holomorphic (3,0) volume form on X. Note that (2.5) depends non-linearly on h. It was shown by Tian [41] that metrics on ample line bundles, such as (2.4), can provide a useful "basis" of Kahler metrics on X. That is, any algebraic Kähler potential can either be written in the form (2.4) or obtained as the limit point of a sequence of such potentials. Specifically, one has the following theorem.

Theorem 1 (Tian). *Let $\{s_\alpha\}$ be a basis for $H^0(X, \mathcal{L}^k)$ for some ample line bundle $\mathcal{L}$. Then the space of all "algebraic" Kähler potentials,*

$$K_{h,k} = \frac{1}{k\pi} \ln \sum_{\alpha,\bar{\beta}=0}^{n_k-1} h^{\alpha\bar{\beta}} s_\alpha \bar{s}_{\bar{\beta}} \tag{2.7}$$

where $k \in \mathbb{Z}$, is dense in the space of Kähler potentials.

With this observation, we return to the goal of finding the Ricci-flat metric on X. Consider X as a projective manifold, with an ample line bundle $\mathcal{L}$. Note that, in general, the matrices $h^{\alpha\bar{\beta}}$ and $M_{\alpha\bar{\beta}}$ in (2.5) are completely unrelated. However, for special metrics, they may coincide. The metric h on the line bundle $\mathcal{L}$ is called *"balanced"* if

$$(M_{\alpha\bar{\beta}})^{-1} = h^{\alpha\bar{\beta}}. \tag{2.8}$$

In this case, one can find an "orthonormal" basis of sections for which $M_{\alpha\bar{\beta}} = \delta_{\alpha\bar{\beta}}$ and $h^{\alpha\bar{\beta}} = \delta^{\alpha\bar{\beta}}$. Many theorems have been proven about balanced metrics. Of particular interest here is their curvature properties [38, 39, 40].

Theorem 2 (Donaldson). *For each $k \geq 1$, the balanced metric, h, on $\mathcal{L}^k$ exists and is unique. As $k \to \infty$, the sequence of metrics*

$$g^{(k)}_{i\bar{j}} = \frac{1}{k\pi} \partial_i \bar{\partial}_{\bar{j}} \ln \sum_{\alpha,\bar{\beta}=0}^{n_k-1} h^{\alpha\bar{\beta}} s_\alpha \bar{s}_{\bar{\beta}} \tag{2.9}$$

on X converges to the unique Ricci-flat metric for the given Kähler class and complex structure.

The core of Donaldson's algorithm is then simply the task of finding the balanced metric for each k. To this end, Donaldson defines the "T-operator"

$$T(h)_{\alpha\bar{\beta}} = \frac{n_k}{\mathrm{Vol}_{CY}(X)} \int_X \frac{s_\alpha \bar{s}_{\bar{\beta}}}{\sum_{\gamma\bar{\delta}} h^{\gamma\bar{\delta}} s_\gamma \bar{s}_{\bar{\delta}}} \, \mathrm{dVol}_{CY} \tag{2.10}$$

which, for a metric h, computes the matrix $T(h)$. Given a fixed point of this operator, that is, a metric h for which $T(h) = h$, one can always perform a change of basis $s \to h^{-1/2} s$ to bring h to the unit matrix, producing a balanced embedding. To find this fixed point, simply iterate (2.10) as follows.

Theorem 3 (Donaldson)**.** *For any initial metric h_0 (and basis s_α of global sections of $\mathcal{L}^k$), the sequence*

$$h_{n+1} = (T(h_n))^{-1} \tag{2.11}$$

converges to the balanced metric as $n \to \infty$.

Happily, in practice, very few (≤ 10) iterations are needed to approach the fixed point. Henceforth, we will also refer to $g^{(k)}_{i\bar{j}}$ in (2.9), the approximating metric for fixed k, as a balanced metric.

To find the balanced metric at each step k, one must be able to integrate over the Calabi-Yau threefold. An explicit numerical integration scheme for this purpose was given in [48, 49] and is used to compute the Calabi-Yau metrics in this paper. We refer the reader to these references for details of this and other technical aspects of the computer implementation. To summarize Donaldson's algorithm:

1. Choose an ample line bundle $\mathcal{L}$ and a degree k (that is, a twisting of the line bundle $\mathcal{L}^k$) at which to compute the balanced metric which will approximate the Calabi-Yau metric.

2. Calculate a basis $\{s_\alpha\}_{\alpha=0}^{n_k-1}$ for $H^0(X, \mathcal{L}^k)$ at the chosen k.

3. Choose an initial non-singular, hermitian matrix, $h^{\gamma\bar{\delta}}$. Perform the numerical integration to compute the T-operator in (2.10).

4. Set the new $h^{\alpha\bar{\beta}}$ to be $h^{\alpha\bar{\beta}} = (T_{\alpha\bar{\beta}})^{-1}$.

5. Return to item 3 and repeat until $h^{\alpha\bar{\beta}}$ approaches its fixed point. In practice, this convergence occurs in less than 10 iterations and does not depend on the initial choice of $h^{\alpha\bar{\beta}}$.

We now turn our attention to how one can measure convergence in Donaldson's algorithm. That is, for each finite step k, how does one define the error measure which tells us how close we are to the unique Ricci-flat metric?

2.2 Ricci Curvature and Error Measures

We begin by defining the Calabi-Yau volume form and several other useful quantities. Let X be a smooth Calabi-Yau variety of dimension d, and let Ω denote the unique (up to a constant) $(d, 0)$ form. The associated volume is given by

$$\mathrm{Vol}_{CY} = \int_X \Omega \wedge \overline{\Omega} \, . \tag{2.12}$$

Given an ample line bundle $\mathcal{L}$, let ω_k denote the Kahler form

$$\omega_k = \frac{i}{2} g^{(k)}_{i\bar{j}} dz_i \wedge d\bar{z}_{\bar{j}} \tag{2.13}$$

of the balanced metric associated with $\mathcal{L}^k$. Note that the Kähler class associated with this Kähler form is $[\omega_k] = 2\pi c_1(\mathcal{L}^k)$. The associated volume is

$$\mathrm{Vol}_k = \frac{1}{d!}\int_X \omega_k^d \ , \tag{2.14}$$

where ω_k^d denotes the (d,d) volume form $\omega \wedge \cdots \wedge \omega$. As expected, when numerically computed, this value is close to $k^d \int_X \omega_1^d$. If, for example, we restrict to the case of the degree $d+2$ hypersurface in $\mathbb{P}^{d+1}$, then by Poincare duality we have that

$$\int_X \omega_1^d = (d+2)\int_{\mathbb{P}^{d+1}} \left(\omega_1^{\mathbb{P}^{d+1}}\right)^d , \tag{2.15}$$

which allows us to fix the overall normalization to $\int_X \omega_1^d = d+2$.

These two volumes allow one to define several measures of the convergence of the balanced metric to the Ricci-flat metric. The first is σ_k introduced in [48, 49] and given by

$$\sigma_k = \frac{1}{\mathrm{Vol}_{CY}}\int_X \left|1 - \frac{\omega_k^d/\mathrm{Vol}_k}{\Omega\wedge\overline{\Omega}/\mathrm{Vol}_{CY}}\right| \mathrm{dVol}_{CY} \ . \tag{2.16}$$

Note that the Kähler form in (2.13) is the Calabi-Yau Kähler form if and only if ω_k^3 is proportional to $\Omega\wedge\overline{\Omega}$. Since we know the exact volume form $\Omega\wedge\bar{\Omega}$, only ω_k is approximate in (2.16) and depends on the degree of k. Hence, the integral in (2.16) vanishes if and only if ω_k is the Calabi-Yau Kähler form. As k is increased in Donaldson's algorithm, σ_k should approach zero. In [48, 49], there is a prediction as to how σ_k should converge to zero. They find that the error approaches zero at least as rapidly as

$$\sigma_k = \frac{a_2}{k^2} + \frac{a_3}{k^3} + \ldots \tag{2.17}$$

for some constants a_i. This prediction is verified by our results in the next subsection.

The second error measure we use is a global measure of convergence for the Ricci scalar,

$$||R||_k = \frac{\mathrm{Vol}_k^{1/d}}{\mathrm{Vol}_{CY}}\int |R_k| \ \mathrm{dVol}_k \ . \tag{2.18}$$

R_k is the Ricci scalar computed with the balanced metric ω_k and we integrate its absolute value. Note that by including the factor $\mathrm{Vol}_k^{1/d}$, the naive linear k dependence of the integral inherited from the fact that $c_1(\mathcal{L}^k) = kc_1(\mathcal{L})$ is canceled. As the balanced metrics converge to the Ricci-flat metric for increasing k, this measure should approach zero.

Third, instead of using the exact Calabi-Yau volume form, one can also use the volume-form computed from the approximate Calabi-Yau metric. This is nothing but the Einstein-Hilbert action, so we define

$$EH_k = \mathrm{Vol}_k^{(1-d)/d}\int R_k \ \frac{\omega_k^d}{d!} = \mathrm{Vol}_k^{(1-d)/d}\int R_k \ \sqrt{\det g_k}\ \mathrm{d}^{2d}x \ . \tag{2.19}$$

Note, however, that on a Kähler manifold the closed two-form $\mathrm{Ric} = R_{i\bar{j}}\,\mathrm{d}z^i\,\mathrm{d}\bar{z}^{\bar{j}}$ defines the first Chern class of X, since $c_1(X) = [\frac{Ric}{2\pi i}]$. Furthermore, $\mathrm{Ric}\wedge\omega^{d-1} = 2dR\omega^d$ and hence, the Einstein-Hilbert action

$$EH_k = \mathrm{Vol}_k^{(1-d)/d}\int_X R_k\;\omega^d = \mathrm{Vol}_k^{(1-d)/d}\int_X c_1(X)\wedge\frac{\omega^{d-1}}{d!} = 0 \tag{2.20}$$

vanishes on a Calabi-Yau manifold for any metric (and hence for any integer k). As a result, we can use this to directly test the accuracy of our numerical integration. However, a better measure of the convergence of the balanced metrics to the Ricci-flat metric is given by

$$||EH||_k = \mathrm{Vol}_k^{(1-d)/d}\int |R_k|\;\sqrt{\det g_k}\;\mathrm{d}^{2d}x\;. \tag{2.21}$$

On a Calabi-Yau manifold, $||R||_k, ||EH||_k = O(k^{-1})$ as $k\to\infty$ and, hence, these error measures should approach zero.

2.3 The Quartic $K3$

In the next two subsections, we use the algorithm outlined above to numerically compute the Ricci-flat metric on two Calabi-Yau manifolds. Two separate computer implementations of Donaldson's algorithm were developed in [48, 49] and [50, 43]. We have utilized these two independent sets of code to check the accuracy of our results. These will be denoted as `Code1` and `Code2` respectively in the following.

Begin with the simple case of the $K3$ twofold. In this subsection, we consider the one parameter deformation X of the Fermat quartic in $\mathbb{P}^3$ given by

$$X: \quad \sum_{i=0}^{3} z_i^4 - 4\psi\prod_{i=0}^{3} z_i = 0. \tag{2.22}$$

Here $z_0,\ldots z_3$ are the homogeneous coordinates on $\mathbb{P}^3$. The deformation parameter ψ is, on the face of it, a complex number. However, redefining

$$\psi\mapsto e^{2\pi i/4}\psi, \quad \big[z_0:z_1:z_2:z_3\big]\mapsto\big[\mapsto e^{-2\pi i/4}z_0:z_1:z_2:z_3\big] \tag{2.23}$$

leaves X invariant, leading to a $\mathbb{Z}_4$ isometry acting on the naive modulus ψ. In other words, the actual modulus is ψ^4, and the complex structure moduli space has an orbifold singularity at the Fermat point $\psi = 0$. As is well known, the algebraic variety X is smooth as long as ψ is not a fourth root of unity and is away from the large complex structure limit, that is, $\psi^4\neq 1,\infty$.

The very ample line bundle we consider is $\mathcal{L} = \mathcal{O}_X(1)$. For each k, we computed the quantities in question for both $\psi = 0.5$ and $\psi = 0.5e^{2\pi i/4}$. These two parameter

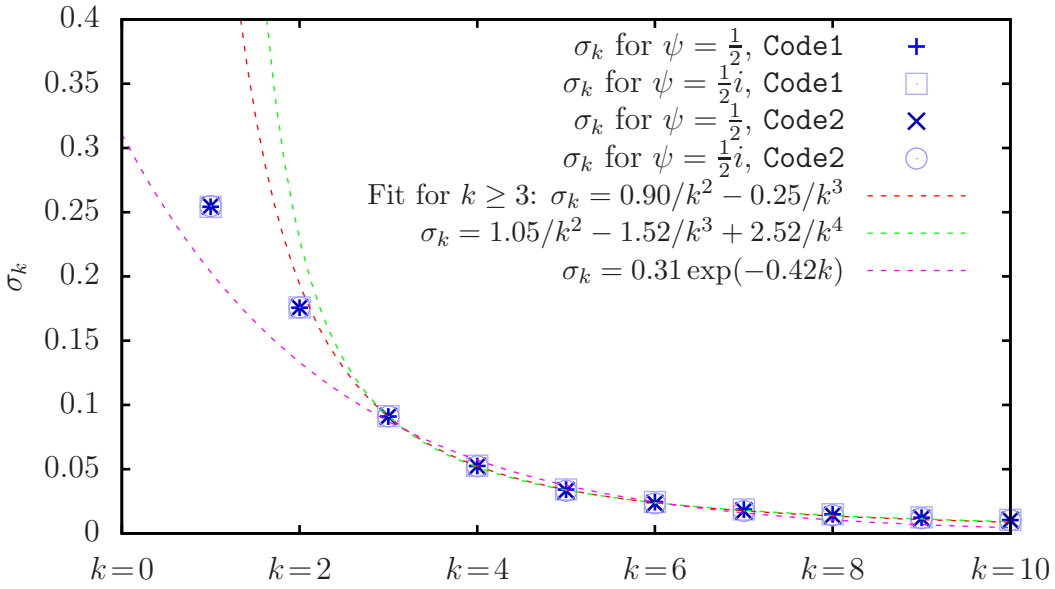

Figure 1: *The error measures σ_k defined in Subsection 2.2. The data shown is for the Quartic K3 defined as a hypersurface in $\mathbb{P}^3$ (2.22). The complex structure parameter is chosen to be $\psi = \frac{1}{2}$ and $\psi = \frac{i}{2}$. Shown is data generated using the code developed in [48, 49] (`Code1`) and data generated by the implementation in [50, 43] (`Code2`). The error measure is fitted to the theoretical convergence given in* (2.17).

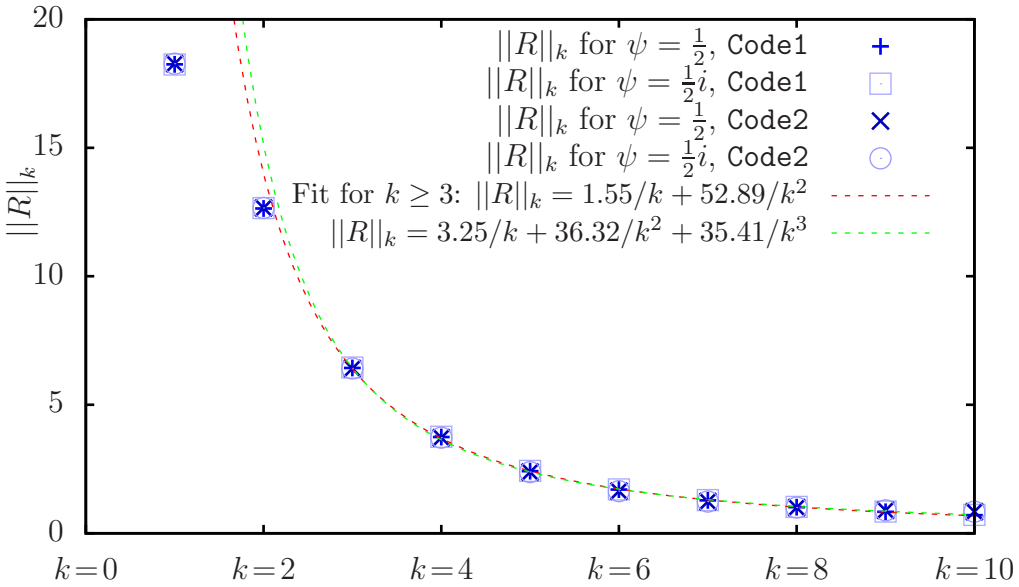

Figure 2: *Average scalar curvature for the metric on $K3 \subset \mathbb{P}^3$.*

values are a significant check of the validity of our numerical implementation since these two $K3$ metrics are, in fact, identified under the $\mathbb{Z}_4$ discrete isometry of X. We would expect the metric results for these two values of ψ to be identical up to numerical errors. This is confirmed by the data shown in Figures 1, 2, and 3.

In these plots, the T-map was iterated with 1,600,000 points, and the error measures were computed with 500,000 points. The high accuracy allows one to conclude that both code bases give the same result. Moreover, especially for high k the assumption that $\sigma_k = O(\frac{1}{k})$ fits our data better than exponential fall-off, see [49, 46].

2.4 The Quintic Threefold

Now consider a Calabi-Yau threefold; specifically, the one parameter deformation X of the Fermat quintic in $\mathbb{P}^4$ given by

$$X\colon \sum_{i=0}^{4} z_i^5 - 5\psi \prod_{i=0}^{4} z_i = 0 \ . \tag{2.24}$$

The algebraic variety X is smooth as long as ψ is not a fifth root of unity. The T-map was iterated with 2,000,000 points, and the error measures were computed with 500,000 points.

The very ample line bundle we consider is again $\mathcal{L} = \mathcal{O}_X(1)$. For each k, we computed the quantities in question for both $\psi = 0.5$ and $\psi = 0.5e^{2\pi i/4}$. As described in the previous subsection, due to the discrete $\mathbb{Z}_5$ isometry of the quintic given in (2.24), we would expect the metric results to be identical for these two choices. Once again, this is verified by the plots in Figure 4 and 5. We also repeated the computation of $||EH||_k$ compared to $||R||_k$. The result is shown in Figure 6. As discussed in the Subsection 2.2, using the identity in (2.20) one can estimate the accuracy of the numerical integration from $EH_k \approx 0$.

3 Hermitian Yang-Mills Connections

3.1 Generalizing Donaldson's Algorithm

As we saw in the previous section, Donaldson's algorithm is a powerful tool for numerically approximating the Calabi-Yau metric. In this section, we investigate a generalization of these techniques which can be used to approximate the field strength, $F^{(1,1)}$, of a holomorphic connection which satisfies (1.13). As discussed in Section 2, Donaldson's algorithm can be viewed as a method for numerically obtaining a particular Hermitian structure on the ample line bundle $\mathcal{L}^k$, see (2.5). This "balanced" fiber metric on $\mathcal{L}^k$ allows one to define a balanced embedding of the Calabi-Yau space X into $\mathbb{P}^{n_k-1}$. By mapping the coordinates $x \in X$ into the global sections $s_\alpha \in H^0(X, \mathcal{L}^k)$,

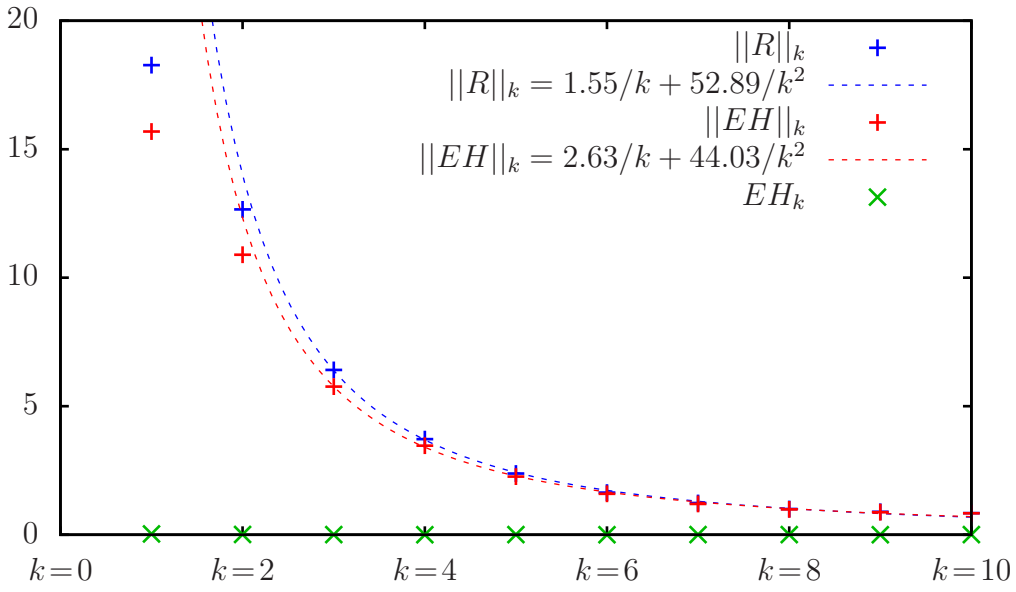

Figure 3: *Curvature measures for $K3 \subset \mathbb{P}^3$. These provide the additional checks of numeric accuracy described in Subsection 2.2.*

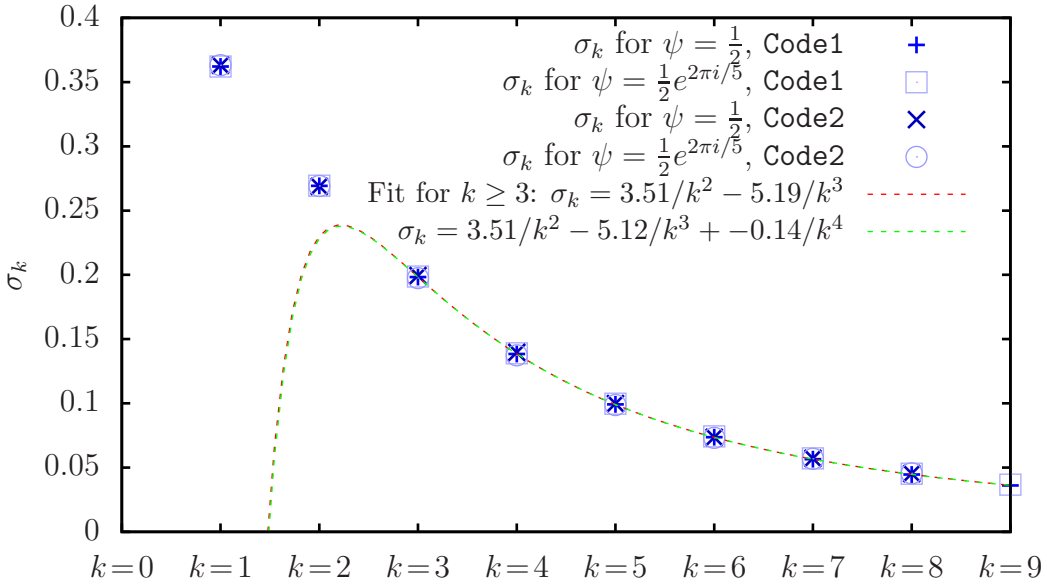

Figure 4: *The σ_k error measures for the quintic threefold (2.24) in $\mathbb{P}^4$. Shown is the error measure described in Subsection 2.2, evaluated for the two values $\psi = \frac{1}{2}$ and $\psi = \frac{i}{2}$. `Code1` and `Code2` are associated to the implementations of [48, 49] and [50, 43] respectively.*

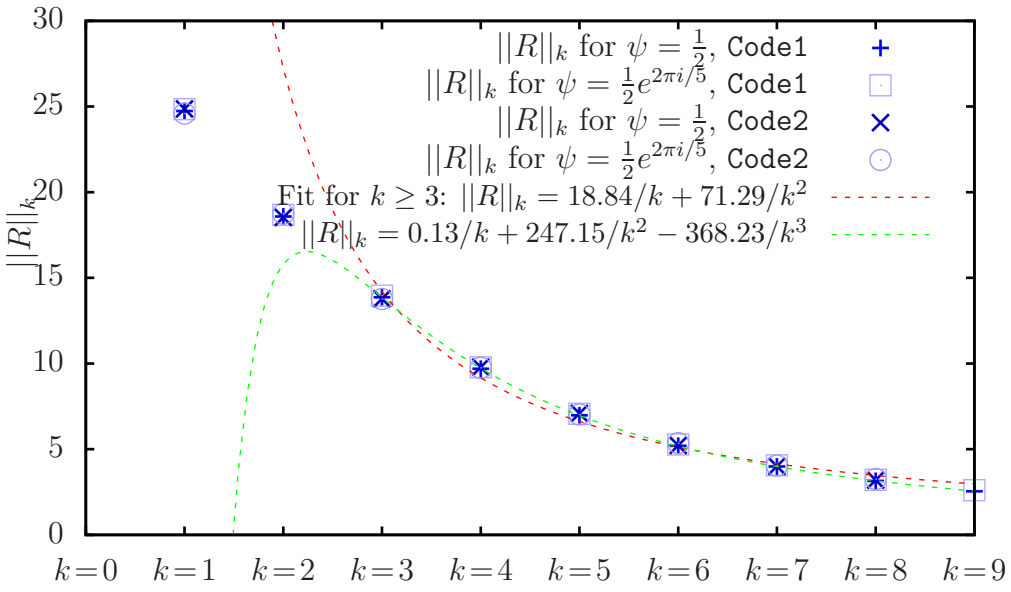

Figure 5: *Average scalar curvature for the metric on the Quintic,* (2.24).

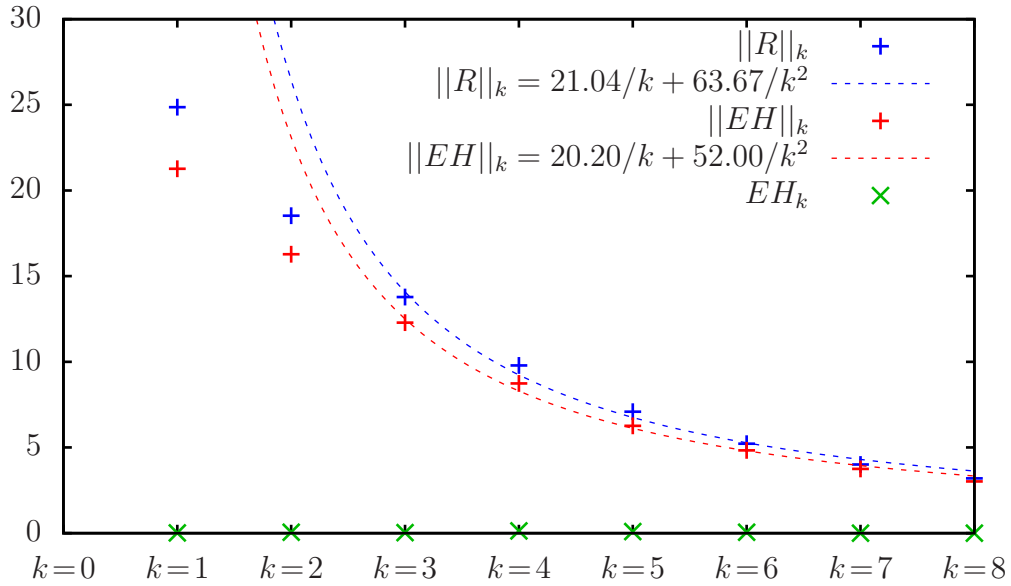

Figure 6: *Curvature measures for the Quintic,* (2.24).

that is,

$$x \longmapsto [s_0(x) : \cdots : s_{n_k-1}(x)] \ , \tag{3.1}$$

we produce a map $i_k : X \to \mathbb{P}^{n_k-1} = G(1, n_k - 1)$ where $n_k = h^0(X, \mathcal{L}^k)$. The pull-back of the associated Fubini-Study metric was shown in Subsection 2.1 to converge to the Ricci-flat metric on X in the limit that $k \to \infty$. It is a natural question to ask whether or not an analogous algorithm could be developed to approximate Hermitian metrics on higher rank vector bundles? In particular, could one find an approximation scheme to produce an Hermitian metric on an arbitrary stable bundle $\mathcal{V}$ of rank n such that it satisfies condition (1.8)? Fortunately, precisely this question has been addressed in the mathematics literature [42] and in [43].

To begin a generalization of Donaldson's algorithm, consider defining an embedding via the global sections of a twist of some holomorphic vector bundle, $\mathcal{V}$, with non-Abelian structure group. That is, consider a map

$$x \longmapsto \left[\begin{pmatrix} S_1^1(x) \\ \vdots \\ S_1^n(x) \end{pmatrix} : \cdots : \begin{pmatrix} S_{N_k}^1(x) \\ \vdots \\ S_{N_k}^n(x) \end{pmatrix} \right] . \tag{3.2}$$

from the coordinates, x, of X into the global sections $S_\alpha^a \in H^0(X, \mathcal{V} \otimes \mathcal{L}^k)$, where $\alpha = 0 \ldots N_k - 1 = h^0(X, \mathcal{V} \otimes \mathcal{L}^k)$ (the number of global sections of $\mathcal{V} \otimes \mathcal{L}^k$) and the index $a = 1, \ldots n$ is valued in the fundamental representation of structure group $K \subset U(n)$ of the rank n bundle $\mathcal{V}$. We hope then to define the embedding

$$X \to G(n, N_k - 1) \ , \tag{3.3}$$

where $G(n, N_k - 1)$ denotes the Grassmannian of the relevant dimension. By the Kodaira embedding theorem [61], given a holomorphic vector bundle $\mathcal{V}$ and an ample line bundle $\mathcal{L}$, there must exist a finite integer k_0 such that, for any $k > k_0$, a "twist" of the bundle $\mathcal{V}(k) = \mathcal{V} \otimes \mathcal{L}^k$ defines an embedding, $i_k : X \to G(n, N_k - 1)$.

Such twisting is a clear necessary for the bundles of interest in $E_8 \times E_8$ heterotic compactifications. Because a slope-stable bundle $\mathcal{V}$ in a heterotic compactification cannot have any global sections[1], $H^0(X, \mathcal{V}) = 0$, we begin by twisting the bundle by some sufficiently large power of an ample line bundle $\mathcal{L}$. That is, we consider $\mathcal{V} \otimes \mathcal{L}^k$. If $\mathcal{L}$ is ample, then $\mathcal{V} \otimes \mathcal{L}^k$ will be generated by its global sections; that is, it will define an embedding as in (3.3). In our search for a solution to the Hermitian Yang-Mills equation (1.13), the connection on the twisted bundle will be closely related to the original connection, since such a twist only modifies the trace part of the field

[1]To see why this is the case, note that for the structure group K of $\mathcal{V}$ to embed inside E_8 one must require that $K = SU(n)$ for $n = 3, 4, 5$ and, hence, that $c_1(\mathcal{V}) = 0$. Therefore, from (1.10) it follows that $\mu(\mathcal{V}) = 0$. However, if $H^0(X, \mathcal{V}) \neq 0$ then $\mathcal{O}_X$ must inject into $\mathcal{V}$ in contradiction with the assumption of stability.

strength. Stated in terms of algebraic geometry, the process of twisting will not modify the slope-stability properties of $\mathcal{V}$ since $\mathcal{V} \otimes \mathcal{L}^k$ is stable if and only if $\mathcal{V}$ is.

As at the beginning of Subsection 2.1, where we chose the trial form of the Kähler potential in (2.4), here we begin with another simple anzatz; this time, however, for the Hermitian structure G in (1.4). We consider an Hermitian matrix $(G^{-1})^{a\bar{b}}$ of the form

$$(G^{-1})^{a\bar{b}} = \sum_{\alpha,\beta=0}^{N_k-1} H^{\alpha\bar{\beta}} S^a_\alpha (\bar{S})^{\bar{b}}_{\bar{\beta}} \ , \tag{3.4}$$

where $H^{\alpha\bar{\beta}}$ is an arbitrary matrix and S^a_α are the global sections of $\mathcal{V} \otimes \mathcal{L}^k$. As in (1.9), this fiber metric induces an inner product on the space of sections, S^a_α, given by

$$< S_\beta | S_\alpha >= \frac{N_k}{\mathrm{Vol}_{CY}} \int_X S^a_\alpha (G^{a\bar{b}})^{-1} \bar{S}^{\bar{b}}_{\bar{\beta}} \, \mathrm{dVol}_{CY} = \frac{N_k}{\mathrm{Vol}_{CY}} \int_X S^a_\alpha (S^a_\gamma H^{\gamma\bar{\delta}} \bar{S}^{\bar{b}}_{\bar{\delta}})^{-1} \bar{S}^{\bar{b}}_{\bar{\beta}} \, \mathrm{dVol}_{CY} \ . \tag{3.5}$$

With this definition of the inner product on sections, one can give a natural generalization of the T-operator (2.10). This generalization,

$$T(H)_{\alpha\bar{\beta}} = \frac{N_k}{\mathrm{Vol}_{CY}} \int_X S_\alpha \Big(S^\dagger H S \Big)^{-1} \bar{S}_{\bar{\beta}} \, \mathrm{dVol}_{CY} \ , \tag{3.6}$$

was introduced in [42] and studied numerically in [43]. Note that when $\mathcal{V}$ is a line bundle, (3.6) reduces to (2.10) and we return to the case of a balanced embedding into $\mathbb{P}^{N_k-1}$. As in the previous section, we will describe how the iteration of the generalized T-operator can produce a fixed point which describes an Hermitian-Einstein bundle metric.

In [42], it was shown that the bundle $\mathcal{V}$ is Gieseker stable[2] if and only if the k-th embedding (defined by $\mathcal{V} \otimes \mathcal{L}^k$ as in (3.3)) can be moved to a "balanced" place. That is, if there exists an orthonormal section-wise metric on the twisted bundle such that

$$(T(H)_{\alpha\bar{\beta}})^{-1} = H^{\alpha\bar{\beta}} \tag{3.8}$$

is a fixed point of the generalized T-operator We can use this special metric on $\mathcal{V} \otimes \mathcal{L}^k$ to define an Hermitian metric on $\mathcal{V}$ itself. Let $G_{\mathcal{L}}$ denote the Hermitian metric on $\mathcal{L}$ and $G^{(k)}$ the balanced metric on $\mathcal{V} \otimes \mathcal{L}^k$. Then

$$G_k = G^{(k)} \otimes G_{\mathcal{L}}^{-k} \tag{3.9}$$

is an Hermitian metric on $\mathcal{V}$. This appears in the following important theorem [42].

[2]Let $\mathcal{L}$ be an ample line bundle. For any torsion-free sheaf $\mathcal{F}$ define the Hilbert polynomial with respect to $\mathcal{L}$ as

$$p_{\mathcal{L}}(\mathcal{F})(n) = \frac{\chi(\mathcal{F} \otimes \mathcal{L}^n)}{rank(\mathcal{F})} \tag{3.7}$$

where $\chi(\mathcal{F} \otimes \mathcal{L}^n)$ is the index of $\mathcal{F} \otimes \mathcal{L}^n$. Given two polynomials f and g, we will write $f \prec g$ if $f(n) < g(n)$ for all $n \gg 0$. Then a bundle $\mathcal{V}$ is said to be Gieseker stable if for every non-zero torsion free subsheaf $\mathcal{F} \subset \mathcal{V}$, $p_{\mathcal{L}}(\mathcal{F}) \prec p_{\mathcal{L}}(\mathcal{V})$ [54].

Theorem 4 (Wang)**.** *Suppose $\mathcal{V}$ is a rank n, Gieseker stable bundle. If $G_k \to G_\infty$ as $k \to \infty$, then the metric G_∞ solves the "weak Hermite-Einstein equation"*

$$g^{i\bar{j}} F_{i\bar{j}} = \left(\mu + \frac{\overline{R} - R}{2}\right) \mathbf{1}_{n\times n} \tag{3.10}$$

where

- *R is the scalar curvature.*
- *$\overline{R} = \int R\sqrt{\det g}\; d^{2d}x$. This vanishes (for any Kähler metric) on a manifold with vanishing first Chern class.*

Procedurally, the process of obtaining the Hermitian-Einstein fiber metric on a slope-stable bundle, $\mathcal{V}$, is very similar to that outlined for the Ricci-flat connection in Section 2 - for each value k of the twisting, we iterate the T-operator associated with the embedding defined by $H^0(X, \mathcal{V}\times\mathcal{L}^k)$ until a fixed point is reached. Then, by Theorem 4, in the limit that $k \to \infty$ the induced connection solves (3.10). However, there is an immediate and important difference between this generalized algorithm and Donaldson's algorithm for Ricci-flat metrics. Note that while all slope-stable bundles are Gieseker stable [54], the converse does not hold–not all Gieseker bundles are slope-stable. That is, there certainly exist cases where the iteration of the T-operater *does not* converge (at a given k). However, if $\mathcal{V}$ is a slope-stable holomorphic bundle, then the iteration $H_{n+1} = T(H_n)^{-1}$ *will* converge at each k, and in the limit that $k \to \infty$, produce the Hermitian bundle metric G_∞ satisfying (3.10) (via its associated field strength defined in (1.7) and (1.8)). Moreover, in the case where the Calabi-Yau metric $g^{i\bar{j}}$ is Ricci-flat, (3.10) simply reduces to (1.13). Thus, we have found a solution to the standard Hermitian-Einstein equations.

3.2 Untwisting

Despite having described a balanced embedding associated with the twisted bundle $\mathcal{V}\otimes\mathcal{L}^k$, and an Hermitian metric G_∞ satisfying (3.10), our task is not yet complete. Thus far, the discussion has been completely general and could be applied to any stable $U(n)$ bundle. However, for the physics associated with an $E_8 \times E_8$ heterotic string theory, we are ultimately interested in the explicit connection, A, on the $SU(n)$ bundle $\mathcal{V}$ itself satisfying the slope-zero Hermitian Yang-Mills equations, (1.1). Since the process of twisting $\mathcal{V}$ by a line bundle $\mathcal{L}^k$ in the above construction clearly modifies the trace-part of the connection, one must subtract this line bundle contribution to get the connection on $\mathcal{V}$ *only*. To do this, we have to separately compute the balanced metric, $G_\mathcal{L}$, on $\mathcal{L}$.

Each of the bundle metrics, $G_\mathcal{L}$ on $\mathcal{L}$ and $G^{(k)}$ on $\mathcal{V}\otimes\mathcal{L}^k$, as well as the Calabi-Yau metric $g^{i\bar{j}}$ must be approximated numerically. The computation of the Hermitian Yang-Mills connection in (1.1) rests on three finite-dimensional approximations:

1. The degree k_g at which we compute the metric,

2. The degree k_H used to compute the twisted connection

3. The degree k_h used to compute the $U(1)$ part of the connection that must be subtracted to obtain the final $SU(n)$ connection on $\mathcal{V}$.

Since the Hermitian Yang-Mills connections are unique (for a given choice of Calabi-Yau metric and geometric moduli), if we can approximate the connections on $\mathcal{V} \otimes \mathcal{L}^{k_H}$ and $\mathcal{L}^{k_h}$ with sufficient accuracy, then we can compute them numerically in a completely independent way. In terms of the metrics on $\mathcal{V} \otimes \mathcal{L}^{k_H}$ and $\mathcal{L}^{k_h}$, we must find

- the metric on $\mathcal{V} \otimes \mathcal{L}^{k_H}$, $G^{(k_H)} = (S^\dagger H S)$, where k_H denotes the finite number of iterations that will be performed to compute the connection.

- the metric on $\mathcal{L}^{k_h}$, $(G_{\mathcal{L}})^{k_h} = (s^\dagger h s)$ (and hence $G_{\mathcal{L}} = (s^\dagger h s)^{1/k_h}$), where k_h will denote the number of iterations to approximate the connection.

Then, as in (3.9) we find that

$$G = G^{(k_H)} \times G_{\mathcal{L}}^{-k_H} = \Big(S^\dagger H S\Big)\Big(s^\dagger h s\Big)^{-k_H/k_h} \tag{3.11}$$

is the fiber metric (1.4) on $\mathcal{V}$. As before, $S \in H^0(X, \mathcal{V} \otimes \mathcal{L}^{k_H})$ and $s \in H^0(X, \mathcal{L}^{k_h})$.

Using (1.7) and (1.8), in terms of the Hermitian metric the connection on $\mathcal{V}$ is then simply

$$\begin{aligned} A(\mathcal{V}) &= \partial\left[\Big(S^\dagger H S\Big)\Big(s^\dagger h s\Big)^{-k_H/k_h}\right]\Big(S^\dagger H S\Big)^{-1}\Big(s^\dagger h s\Big)^{k_H/k_h} \\ &= \Big(\partial(S^\dagger H S)\Big)\Big(S^\dagger H S\Big)^{-1} - \frac{k_H}{k_h}\Big(\partial(s^\dagger h s)\Big)\Big(s^\dagger h s\Big)^{-1} \\ &= A(\mathcal{V} \otimes \mathcal{L}^{k_H}) - \frac{k_H}{k_h} A(\mathcal{L}^{k_h}) \ . \end{aligned} \tag{3.12}$$

That is, one can "untwist" the connection simply by subtracting the trace of the $U(n)$ connection to produce an $SU(n)$ connection. The degrees of approximation k_H and k_h can, in principle, be chosen independently, as long as both are sufficiently large. We will discuss the choice of the line bundle $\mathcal{L}$ and twisting degree k_h in more detail in the next subsection.

The curvature is given by

$$F^{(0,2)} = F^{(2,0)} = 0, \quad g^{i\bar{j}} F_{i\bar{j}} = g^{i\bar{j}} \partial_{\bar{j}} A_i = g^{i\bar{j}} \partial_{\bar{j}} \partial_i \ln\Big(S^\dagger H S\Big)\Big(s^\dagger h s\Big)^{-k_H/k_h}. \tag{3.13}$$

In summary, the following is an outline of the computation the Hermitian Yang-Mills connection (that is, the solution to (1.1)).

1. Following Donaldson's algorithm derived in Subsection 2.1, approximate the unique Ricci-flat metric $g^{i\bar{j}}$ on X to the desired degree (determined by k_g, the iteration parameter of Theorem 2, (2.9)).

2. For a given holomorphic vector bundle $\mathcal{V}$, choose an ample line bundle $\mathcal{L}$ on X and a degree k_H (that is, a twisting of the vector bundle $\mathcal{V} \otimes \mathcal{L}^{k_H}$) at which to compute the "balanced" fiber metric (3.8)

3. Calculate a basis $\{S_\alpha\}_{\alpha=0}^{N_{k_H}-1}$ for $H^0(X, \mathcal{V} \otimes \mathcal{L}^{k_H})$ at the chosen k_H.

4. Choose an initial, invertible, Hermitian matrix, $H^{\gamma\bar{\delta}}$ for the ansatz (3.4). Perform the numerical integration to compute the T-operator in (3.6).

5. Set the new $H^{\alpha\bar{\beta}}$ to be $H^{\alpha\bar{\beta}} = (T_{\alpha\bar{\beta}})^{-1}$.

6. Return to item 3 and repeat until $H^{\alpha\bar{\beta}}$ approaches its fixed point. In practice, this convergence occurs in less than 10 iterations and does not depend on the initial choice of $H^{\alpha\bar{\beta}}$. At this point, we have obtained the Hermitian metric on $\mathcal{V} \otimes \mathcal{L}^{k_H}$ to the desired accuracy.

7. Approximate the Hermitian metric on $\mathcal{L}$ to a chosen degree k_h by repeating steps 2 to 6 for $\mathcal{L}^{k_h}$

8. Compute the "untwisted" connection and field strength via (3.12) and (3.13)

We turn now to a discussion of the accuracy of these numerical approximations.

3.3 Measuring the Error

As discussed above, in a computer implementation of the generalized Donaldson's algorithm one must rely on three expansion parameters. Two are associated with the approximation of the balanced Hermitian metrics on $\mathcal{V} \otimes \mathcal{L}^{k_H}$ and $\mathcal{L}^{k_h}$, and the third with the Calabi-Yau metric calculated with parameter k_g. Having implemented this, we would like to know how far our numerical connection for fixed k_g, k_H, k_h deviates from the exact Hermitian Yang-Mills connection (1.1).

$F^{0,2}$ and $F^{2,0}$ are automatically zero with our ansatz (1.7) for the connection. Hence, for an $SU(n)$ bundle we have only to test how far the "color matrix" $g^{i\bar{j}}F_{i\bar{j}}$ deviates from the zero matrix. Note that the matrix entries depend on the chosen frame. Thus the appropriate invariant quantity to consider for such an Hermitian matrix is its (real) eigenvalues

$$g^{i\bar{j}}F_{i\bar{j}} \sim \begin{pmatrix} \lambda_1 & & & \\ & \lambda_2 & & \\ & & \ddots & \\ & & & \lambda_n \end{pmatrix} . \tag{3.14}$$

For an $SU(n)$ bundle, we expect

$$\lambda_i \to 0 \quad \forall \quad i \tag{3.15}$$

if and only if the connection is approaching a solution to (1.1). We begin by investigating the eigenvalues of the "color matrix" at a point. An integrated error measure will be discussed in the next subsection. To illustrate these concepts, we turn to a simple example of a stable bundle.

3.4 An Example

To begin, consider the Quartic $K3$ of Subsection 2.3. We define an explicit such hypersurface in $\mathbb{P}^3$ by

$$\left\{ z_0^4 + z_1^4 + z_2^4 + z_3^4 - 2z_0z_1z_2z_3 = 0 \right\} \subset \mathbb{P}^3_{[z_0:z_1:z_2:z_3]} \ , \tag{3.16}$$

where z_i denote the coordinates of $\mathbb{P}^3$. The Ricci-flat metric on this manifold was computed up to degree $k_g = 10$ in Subsection 2.3 and the results plotted in Figures 1, 2 and 3.

On this Calabi-Yau twofold, we define the following rank 2, holomorphic vector bundle with structure group $SU(2)$. This sample bundle is defined through the so-called "monad" construction [51, 52, 53, 25]

$$0 \longrightarrow \mathcal{O}(-3) \xrightarrow{f} \mathcal{O}(-1) \oplus \mathcal{O}(-1) \oplus \mathcal{O}(-1) \longrightarrow \mathcal{V}_{\text{stable}} \longrightarrow 0 \ . \tag{3.17}$$

Here $\mathcal{V}_{\text{stable}}$ is defined as the cokernel of the map $f = (x_0^2, x_1^2, x_2^2)$ between the direct sums of line bundles. Using the techniques of [54, 62], it is straightforward to prove that $\mathcal{V}_{\text{stable}}$ in (3.17) is slope-stable. Hence, by Theorem 4, we expect the T-operator to converge.

As discussed in Subsection 3.2, to apply the generalized Donaldson algorithm one must define the embedding $i_k : X \to G(n, N_{k_H})$. To do this, we must compute the global sections of the twisted line bundle $\mathcal{V} \otimes \mathcal{L}^{k_H}$ for some ample line bundle $\mathcal{L}$. Fortunately, for the bundle defined in (3.17) the global sections $H^0(X, \mathcal{V} \otimes \mathcal{L}^{k_H})$ can easily be computed as follows. Letting $\mathcal{L}^{k_H} = \mathcal{O}(m)$, from (3.17) we induce the twisted short exact sequence

$$0 \longrightarrow \mathcal{O}(m-3) \xrightarrow{f} \mathcal{O}(m-1)^{\oplus 3} \longrightarrow \mathcal{V}_{\text{stable}} \otimes \mathcal{O}(m) \longrightarrow 0 \ . \tag{3.18}$$

Then the global sections are given simply as the cokernel

$$H^0(X, \mathcal{V} \otimes \mathcal{O}(m)) = \frac{H^0(X, \mathcal{O}(m-1)^{\oplus 3})}{f(H^0(X, \mathcal{V} \otimes \mathcal{O}(m-3)))} \ , \tag{3.19}$$

where both parts of this quotient are the global sections of sums of ample line bundles when $m \geq 3$. Furthermore, on the Quartic $K3$ the global sections of the line bundle $\mathcal{O}(n)$ can be computed as a simple polynomial space of dimension

$$h^0(X, \mathcal{O}(n)) = \begin{cases} 0 & n < 0 \\ \binom{n+3}{3} & 0 \leq n < 4 \\ \binom{n+3}{3} - \binom{n-1}{3} & n \geq 4 \end{cases} \tag{3.20}$$

With these definitions in hand, one can compute a basis of polynomials of $H^0(X, \mathcal{V} \otimes \mathcal{L}^{k_H})$ of the degree given by (3.20).

Following the algorithm developed in the preceeding sections, we first compute $g^{i\bar{j}} F_{i\bar{j}}$ at the randomly chosen point

$$P = \left[1 : 0.707124 + 0.707124i : 0.1 : 0\right] . \tag{3.21}$$

The bundle $\mathcal{V}$ is rank 2, so there are two eigenvalues λ_1, λ_2 in (3.14). Define the following extremal quantities.

$$\begin{aligned} |\lambda|_{\max} &= \max\left\{|\lambda_1|, |\lambda_2|\right\} \\ |\lambda|_{\min} &= \min\left\{|\lambda_1|, |\lambda_2|\right\} . \end{aligned} \tag{3.22}$$

As we iterate the twisting degrees k_H and k_h associated with the connections on $\mathcal{V} \otimes \mathcal{L}^{k_H}$ and $\mathcal{L}^{k_h}$ respectively, we can plot the eigenvalues of (3.14) at the point (3.21). For this example, the connection T-operator was iterated 7 times, numerically integrating over 1,000,000 points. As expected, we find that $\lambda_i \to 0$ as $k_h, k_H \to \infty$. The results are shown in Figure 7. Inspecting this graph, we note several important features. First, observe that the eigenvalues will converge to zero along *any* diagonal ray, that is, in any limit as $k_h, k_H \to \infty$. Second, note that there is clearly some variation in the rate at which the eigenvalues along these rays converge to zero. We will define the optimal choice in the next subsection.

3.5 Subtracting the Trace

As we saw in Subsection 3.2, after twisting up the vector bundle to $\mathcal{V} \otimes \mathcal{L}^{k_H}$ there is a choice in how we compute the connection on the line bundle $\mathcal{L}$. As long as there is some limit (for example, $k_h \to \infty$ and picking the balanced connection) where the connection on the line bundle approaches constant curvature, we will eventually approximate the slope-zero Hermitian Yang-Mills connection on $\mathcal{V}$. Of course, some choices of line bundles work better than others. In this subsection, we discuss the optimal choice–the determinant line bundle of $\mathcal{V} \otimes \mathcal{L}^{k_H}$ with the induced connection. The determinant line bundle is defined as $\wedge^n(\mathcal{V} \otimes \mathcal{L}^{k_H})$. Taking this line bundle as the "untwisting" line bundle and choosing $k_h = \text{rank}(\mathcal{V}) k_H$, we then choose the Hermitian metric

$$(G_{\mathcal{L}})^{k_h} = \det(G^{(k_H)}) = \det\left(S^\dagger H S\right) \tag{3.23}$$

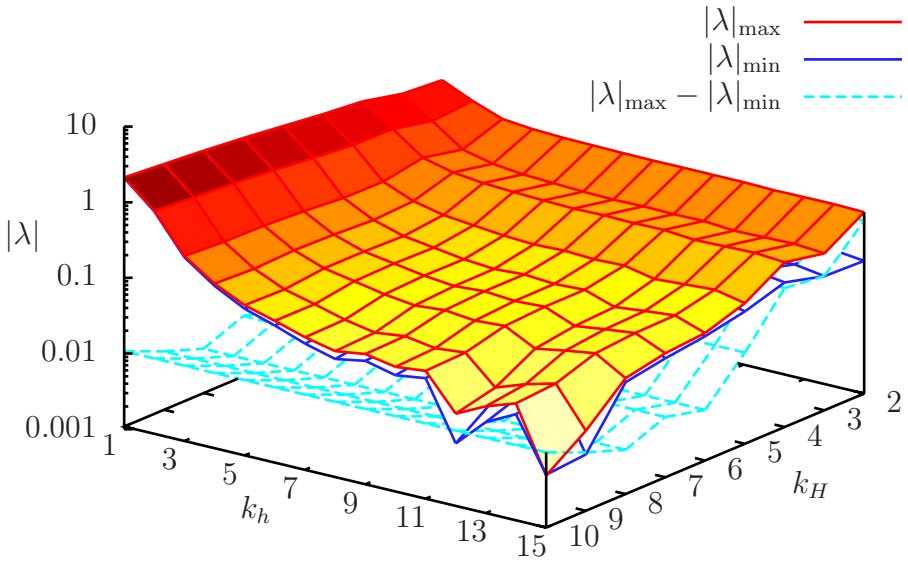

Figure 7: *The eigenvalues of $g^{i\bar{j}}F_{i\bar{j}}(P)$. The actual solution to the Hermitian Yang-Mills connection is characterized by having $\lambda = 0$ at each point. We see that the numerical solution approximates this in the limit as k_H, $k_h \to \infty$.*

on $(\wedge^n(\mathcal{V}\otimes\mathcal{L}^{k_H}))^{k_h}$.

Let $\lambda^{(k_H)}$ be the "twisted" eigenvalues of $g^{i\bar{j}}F^{(k_H)}_{i\bar{j}}$ on $\mathcal{V}\otimes\mathcal{L}^{k_H}$, and let λ be the corresponding eigenvalues of $g^{i\bar{j}}F_{i\bar{j}}$ on $\mathcal{V}$ after "untwisting". Then, from (3.13) we have

$$\lambda_i = \lambda_i^{(k_H)} - \frac{1}{\operatorname{rank}\mathcal{V}} g^{i\bar{j}} \operatorname{tr} F^{(k_H)}_{i\bar{j}} = \lambda_i^{(k_H)} - \frac{\sum_j \lambda_j^{(k_H)}}{\operatorname{rank}\mathcal{V}}. \tag{3.24}$$

Therefore, the effect of this untwisting is precisely to subtract, at each point, the average of the eigenvalues. In this sense, using the determinant line bundle is the optimal way to untwist. Furthermore, with this choice of untwisting, the approximate connection on $\mathcal{V}$ is $SU(n)$ at each value of k_h (as opposed to the other choices for "untwisting" line bundles for which it is only as k_h becomes large that the connection approaches $SU(n)$, see Figure 8). In Figure 8, we compare the untwisting done with various line bundles $\mathcal{L}^{k_h} = \mathcal{O}(1)^{k_h} = \mathcal{O}(k_h)$ on the Quartic with the untwisting by the determinant line bundle. The determinant line bundle clearly produces the most rapid convergence to zero eigenvalues. Therefore, for the remainder of this paper, regardless of the choice of "twisting" line bundle, $\mathcal{L}$, we will always use the determinant line bundle $\wedge^n(\mathcal{V}\otimes\mathcal{L}^{k_H})$ to untwist.

3.6 Integrated Error Measure

To define a true error measure for the approximation to the Hermitian Yang-Mills connection, we must test the approximation at all points (as was done for the error measures for the Ricci-flat metric in Subsection 2.2) and, hence, integrate over X. To do this, define the error measure

$$\tau(A_{\mathcal{V}}) = \frac{1}{2\pi}\frac{k_g}{\operatorname{Vol}_{k_g}\operatorname{rank}(\mathcal{V})}\int_X \Big(\sum|\lambda_i|\Big)\sqrt{g}\,d^{2d}x\ . \tag{3.25}$$

This is simply a global check of the eigenvalues in (3.14). To understand the normalization in (3.25), first note that $g^{i\bar{j}}$ scales as $\frac{1}{k_g}$ with the degree k_g of the metric computation. This explains the prefactor k_g in (3.25). We also divide by the metric volume Vol_{k_g} to cancel the scaling of the volume element $\sqrt{g}$. Finally, observe that

- If all eigenvalues are positive, then $\tau(A_{\mathcal{V}}) = \int c_1(\mathcal{V})\wedge\omega^{D-1} \in \mathbb{Z}$. This is the reason for the prefactor $\frac{1}{2\pi}$, since $[\omega_k] = 2\pi c_1(\mathcal{L}^k)$.
- If $c_1(\mathcal{V}) = 0$, then $\tau_{k_H}(A_{\mathcal{V}}) \longrightarrow 0$ measures convergence to the Hermitian Yang-Mills connection. The eigenvalues must occur with both signs.

Since $c_1(\mathcal{V}\otimes\mathcal{L}^{k_H}) = c_1(\mathcal{V}) + nk_Hc_1(\mathcal{L})$ is the first Chern class of $\mathcal{V}\otimes\mathcal{L}^{k_H}$ (with $n = rank(\mathcal{V})$), we can predict the values of $\tau^{(tw)}_{k_H}$ for the twisted bundle $\mathcal{V}\otimes\mathcal{L}^{k_H}$ as

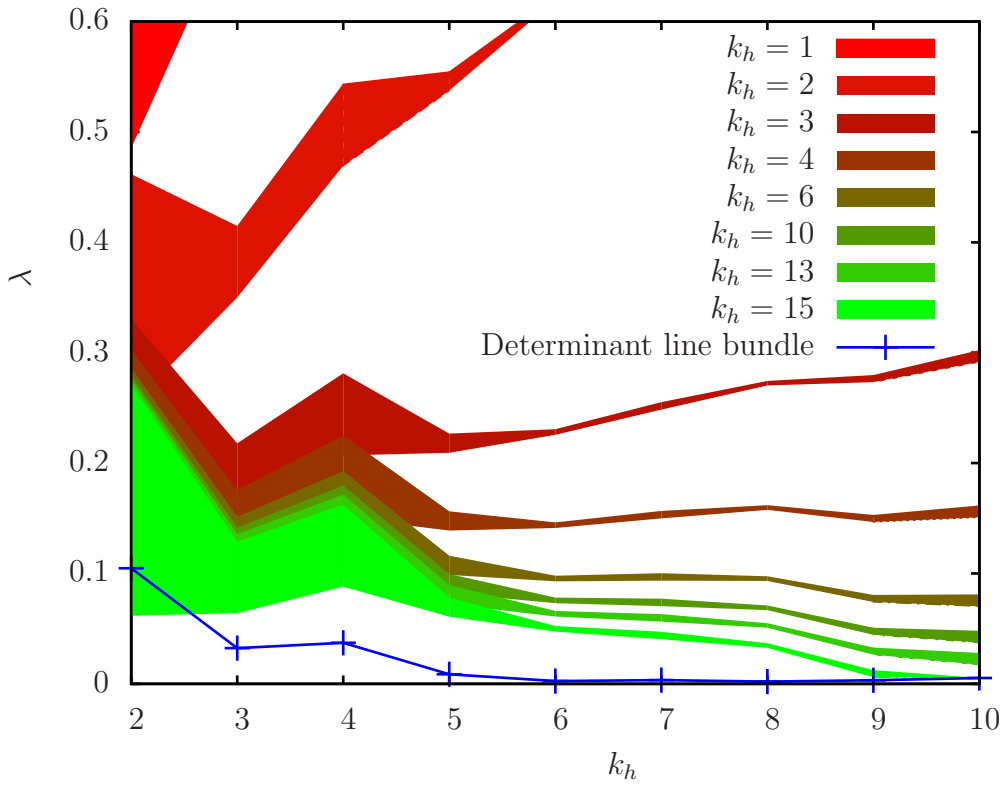

Figure 8: *The eigenvalues of $g^{i\bar{j}}F_{i\bar{j}}(P)$ of the rank 2 bundle $\mathcal{V}$ on the Quartic for different choices of "untwisting line bundle" $\mathcal{L}^{k_h} = \mathcal{O}(1)^{k_h}$ (same data as in Figure 7) as well as the optimal untwisting with the determinant line bundle. The upper and lower boundaries of the colored bars are $|\lambda|_{max}$ and $|\lambda|_{min}$, respectively. In the determinant line bundle case, the two eigenvalues are $\pm\lambda$ and their magnitude is exactly equal at each value of k_h. This magnitude is shown by the blue crosses.*

we increase k_H. Hence, we can learn something from evaluating the τ-integral for the twisted as well as for the untwisted connection. Define

$$\begin{aligned} \tau_{k_H}^{(\mathrm{tw})} &= \tau\big(A_{\mathcal{V}\otimes\mathcal{L}^{k_H}}\big), \\ \tau_{k_H} &= \tau\big(A_{\mathcal{V}\otimes\mathcal{L}^{k_H}} - \tfrac{1}{\mathrm{rank}\,\mathcal{V}} A_{\det(\mathcal{V}\otimes\mathcal{L}^{k_H})}\mathbf{1}_{\mathrm{rank}\,\mathcal{V}}\big), \end{aligned} \tag{3.26}$$

where $\mathbf{1}_{\mathrm{rank}\,\mathcal{V}}$ is the identity matrix in the gauge indices. That is, $\tau_{k_H}^{(\mathrm{tw})}$ is the (properly normalized) integral over the eigenvalues of the twisted-up bundle and τ_{k_H} is the integral over the eigenvalues after untwisting with the determinant line bundle (this expression follows immediately from (3.12) by taking $\mathcal{L}^{k_h} = (\wedge^n(\mathcal{V}\otimes\mathcal{L}^{k_H}))^{rank(\mathcal{V})k_H}$). Note that it implicitly depends on the degree k_g at which we computed the metric. In Table 1, we list both $\tau_{k_H}^{(\mathrm{tw})}$ and τ_{k_H} for the rank 2 bundle defined by (3.17) in

k_H	$\int c_1(\mathcal{V}\otimes\mathcal{L}^{k_H})\wedge\omega$	$\tau_{k_H}^{(\mathrm{tw})}$	τ_{k_H}
2	4	4.00057	0.904183
3	6	6.00329	0.765671
4	8	7.99855	0.532639
5	10	9.99944	0.331912
6	12	12.0012	0.229044
7	14	13.9983	0.170002
8	16	15.9989	0.132257

Table 1: *The integrated error measure for the stable bundle* (3.17) *from Subsection 3.4.* $\tau_{k_H}^{(tw)}$ *before untwisting computes the integral first Chern class. The comparison between the exact value for the integral Chern class and* $\tau_{k_H}^{(tw)}$ *is made in the first two columns. This comparison provides a confirmation of the validity of the algorithm, even before untwisting. In the final column, the error measure for the untwisted bundle is presented.*

Subsection 3.4. In the first column, the integral over the first Chern class of $\mathcal{V}\otimes\mathcal{L}^{k_H}$ is listed, where $\mathcal{L} = \mathcal{O}(1)$ on the $K3$. As expected, $\tau_{k_H}^{(\mathrm{tw})}$ closely matches this value. In the last column, the untwisted error measure is presented. It clearly approaches zero as k_H increases.

In Figure 9, we present our first explicit example of the convergence of the generalized Donaldson algorithm for a slope-stable bundle. We have explicitly computed the field-strength of the $SU(2)$ bundle in (3.17). We find that the associated integrated error measure, τ_{k_H} in (3.25), is converging to zero in the limit that $k_H >> 1$. In addition, in Figure 9 the form of the decreasing τ_{k_H} values is compared with the prediction of an $\sim 1/k_H$ fall-off in the error measure predicted in [42].

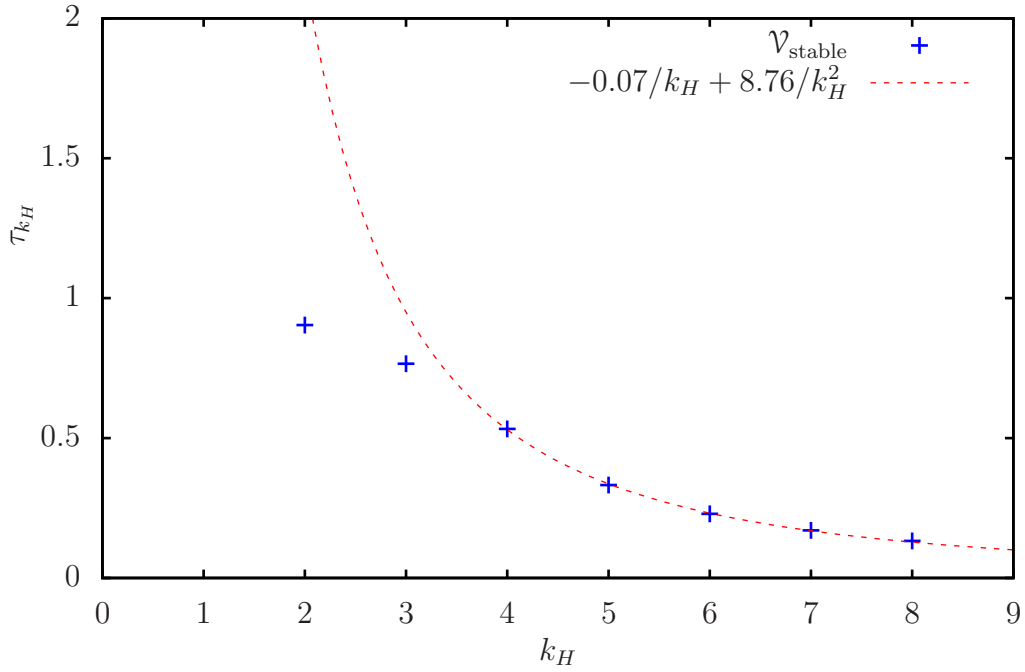

Figure 9: *τ_{k_H} for the stable bundle $\mathcal{V}_{stable}$ defined in* (3.17) *on the Quartic $K3$.*

4 Stable vs. Unstable

In this section, we investigate the behavior of the generalized Donaldson algorithm applied to arbitrary $SU(n)$ vector bundles. This behavior will exhibit more complexity than we encountered in the computation of the Ricci-flat metrics of Section 2. In applying the Donaldson algorithm to the computation of the metric, we are guaranteed that for any compact Kähler manifold X with $c_1(X) = 0$ the Ricci-flat metric exists. Furthermore, the algorithm presented in Subsection 2.1 will approximate it in the limit that $k_g \to \infty$. However, the situation is different for vector bundles. A Hermitian-Einstein metric does not exist for every vector bundle $\mathcal{V}$ on X with $c_1(\mathcal{V}) = 0$. As discussed in Sections 1 and 3.1, the vector bundle must be slope poly-stable for such a Hermitian-Einstein metric to exist. Since this property is difficult to guarantee initially, it seems prudent to ask what behavior we expect to see if we apply this algorithm to bundles that do not, in fact, admit an Hermitian-Einstein fiber metric? In the following, we demonstrate that, surprisingly, the Donaldson algorithm produces distinctive and interesting results even in the case where the bundle is not stable. Furthermore, we will argue that in view of the difficulty in proving slope-stability of vector bundles, *the generalized Donaldson algorithm provides a new and attractive way of numerically deciding whether or not a bundle is stable.*

With this goal in mind, in the next sections we will investigate the slope-stability properties of vector bundles and how this behavior appears in the results of the generalized Donaldson algorithm presented in Subsection 3.1.

4.1 Taxonomy of Slope-Stability

Recall that the slope of a vector bundle $\mathcal{V}$ is defined, with respect to a given Kähler form ω, as

$$\mu(\mathcal{V}) \equiv \frac{1}{\mathrm{rk}(\mathcal{V})} \int_X c_1(\mathcal{V}) \wedge \omega^{d-1}. \tag{4.1}$$

As discussed in Subsection 1.3, there are four possible types of behavior for holomorphic vector bundles. These are [54]

1. **Stable**: An indecomposable bundle, $\mathcal{V}$, is called *stable* if, for all subsheaves $\mathcal{F} \subset \mathcal{V}$, $\mu(\mathcal{F}) < \mu(\mathcal{V})$.

2. **Poly-stable**: A bundle is called *poly-stable* if $\mathcal{V}$ is a direct sum of stable bundles with the same slope: $\mathcal{V} = \bigoplus_i \mathcal{V}_i$ with $\mu(\mathcal{V}_i) = \mu(\mathcal{V})\ \forall\ i$.

3. **Semi-stable**: A bundle is called *semi-stable* if for all subsheaves $\mathcal{F} \subset \mathcal{V}$, $\mu(\mathcal{F}) \leq \mu(\mathcal{V})$. It is *properly* (or strictly) semi-stable if $\mathcal{V}$ is semi-stable but not poly-stable (that is, it is indecomposable).

4. **Unstable**: An *unstable* bundle is one for which $\mu(\mathcal{F}) > \mu(\mathcal{V})$ for at least one proper subsheaf $\mathcal{F} \subset \mathcal{V}$. Unstable bundles can be either decomposable or indecomposable.

Recall that a Hermitian-Einstein metric exists *only* for the first two entries in this list, that is, for poly-stable bundles (stability being a subset of poly-stability).

Before we discuss the results of the generalized Donaldson's algorithm in the four cases above, we must make one further observation about slope-stability. The preceding definitions provide a measure of the degree of substructure present in a given bundle. More precisely, stable bundles are *simple* [54], that is, $H^0(X, \mathcal{V} \otimes \mathcal{V}^\vee) = \mathbb{C}$ and any morphism between two stable bundles $\mathcal{V}_1$,$\mathcal{V}_2$ with $rank(\mathcal{V}_1) = rank(\mathcal{V}_2)$ and $c_1(\mathcal{V}_1) = c_1(\mathcal{V}_2)$ is an isomorphism. Likewise, poly-stable bundles are direct sums of simple objects. But properly semi-stable and unstable objects exhibit a richer structure. Theoretically, there is a natural framework for describing the behavior of semi-stable and unstable vector bundles in terms of a decomposition into simple objects. We discuss this in the next subsection.

4.2 The Harder-Narasimhan Filtration

The following theorem makes explicit how unstable sheaves may be described in terms of semi-stable sheaves, and semi-stable sheaves in terms of stable sheaves [54].

Theorem 5 (Harder-Narasimhan)**.** *Given a holomorphic bundle $\mathcal{V}$ over a closed Kähler manifold X (with Kähler form ω), there is a filtration (called the Harder-Narasimhan filtration) by subsheaves*

$$0 = \mathcal{F}_0 \subset \mathcal{F}_1 \subset \ldots \mathcal{F}_l = \mathcal{V} \tag{4.2}$$

such that $\mathcal{F}_i/\mathcal{F}_{i-1}$ are semi-stable sheaves for $i = 1, \ldots l$ and the slope of the quotients are ordered

$$\mu(\mathcal{F}_1) > \mu(\mathcal{F}_2/\mathcal{F}_1) > \ldots \mu(\mathcal{F}_l/\mathcal{F}_{l-1}) \ . \tag{4.3}$$

If $\mathcal{V}$ is semi-stable, then there is a filtration by subsheaves (called the Jordan-Hölder filtration),

$$0 = \mathcal{F}_0 \subset \mathcal{F}_1 \subset \ldots \mathcal{F}_l = \tilde{\mathcal{V}} \tag{4.4}$$

such that the quotients $\mathcal{F}_i/\mathcal{F}_{i-1}$ are all stable sheaves and have slope $\mu(\mathcal{F}_i/\mathcal{F}_{i-1}) = \mu(\mathcal{V})$. In addition

$$Gr(\mathcal{V}) = \mathcal{F}_1 \oplus \mathcal{F}_2/\mathcal{F}_1 \oplus \ldots \mathcal{F}_l/\mathcal{F}_{l-1} \tag{4.5}$$

is uniquely determined up to isomorphism (and is called the graded sum*).*

One consequence of Theorem 5 is a description of the moduli space of semi-stable sheaves. Two semi-stable bundles $\mathcal{V}_1$ and $\mathcal{V}_2$ are called *S-equivalent* if $Gr(\mathcal{V}_1) = Gr(\mathcal{V}_2)$. The concept of S-equivalence arises when trying to define the notion of a moduli space of sheaves. Stable bundles correspond to unique points in their moduli space, while a moduli space of semi-stable sheaves can only be made Hausdorff if each point corresponds to an S-equivalence class. It is worth observing that each S-equivalence class contains a unique poly-stable representative (namely the graded sum (4.5)).

With these classifying notions in mind, we now return to our discussion of the generalized Donaldson algorithm and the results of the numerical scheme outlined in Subsection 3.1. If we numerically approximate the color matrix $g^{i\bar{j}}F_{i\bar{j}}$ for the four types of bundles described in points 1)-4) above, what will we find? What will be the eigenvalues in (3.14) described in Subsection 3.3, or the behavior of the error measure τ_{k_H} defined by (3.25) in Subsection 3.6?

To answer these questions, we again consider the four types of bundles described in Subsection 4.1 above. Depending on the slope-stability properties of the bundle, the Harder-Narasimhan filtration indicates that there exists a connection which will produce a color matrix $g^{i\bar{j}}F_{i\bar{j}}$ with the following behavior.

1. If $\mathcal{V}$ is a poly-stable (including properly stable) bundle with slope μ, then

$$g^{i\bar{j}}F_{i\bar{j}} \sim \begin{pmatrix} \mu & & \\ & \ddots & \\ & & \mu \end{pmatrix} = \mu(\mathcal{V})\mathbf{1}_{\mathbf{n}\times\mathbf{n}} \ . \tag{4.6}$$

   By Theorem 4, in this case we expect that the generalized Donaldson algorithm will approximate a solution to the Hermitian Yang-Mills equation (1.2).

2. If $\mathcal{V}$ is semi-stable, then, in general, it is not a solution to the Hermitian Yang-Mills equations. The form of its color matrix will depend on the values of the

bundle moduli, $H^1(End(\mathcal{V}))$. These moduli determine where $\mathcal{V}$ is chosen to be within it S-equivalence class. In general, the color matrix $g^{i\bar{j}}F_{i\bar{j}}$ will produce constant, non-equal eigenvalues. However, by varying the bundle moduli, $\mathcal{V}$ can be made arbitrarily close to the unique poly-stable representative (the graded sum (4.5)) in its class. That is, for a properly semi-stable $SU(n)$ bundle, depending on the choice of bundle moduli, the eigenvalues can be made arbitrarily close to zero.

3. If $\mathcal{V}$ is unstable, there are two possible ways in which the field strength fails to satisfy the Hermitian Yang-Mills equations. Either

   (a) Its Harder-Narasimhan filtration (4.2) consists of a sum of bundles (locally free sheaves with constant rank) with inequivalent slopes, μ_i. In this case, the color matrix takes the form

   $$g^{i\bar{j}}F_{i\bar{j}} \sim \begin{pmatrix} \mu_1 & & & \\ & \mu_2 & & \\ & & \ddots & \\ & & & \mu_l \end{pmatrix} . \tag{4.7}$$

   (b) Or its Harder-Narasimhan filtration (4.2) contains torsion-free sheaves (whose rank can change over higher co-dimensional loci in the base X). In this case

   $$g^{i\bar{j}}F_{i\bar{j}} \sim \begin{pmatrix} \mu_1(x) & & & \\ & \mu_2(x) & & \\ & & \ddots & \\ & & & \mu_l(x) \end{pmatrix} , \tag{4.8}$$

   where $\mu_i(x)$ can vary in magnitude over the base X. In particular, at the locus in the base where the rank of $\mathcal{V}$ jumps, $F_{i\bar{j}}$ can diverge to produce a curvature singularity.

How will this behavior appear in the generalized Donaldson algorithm? As stated above, we are guaranteed that the algorithm produces the physical connection only in the case when the vector bundle is stable and the T-operator converges. But we can now ask, what happens when we apply the algorithm to properly semi-stable or unstable bundles? We will explore this experimentally first by looking at sample $SU(n)$ bundles defined on the familiar Quartic $K3$.

4.3 Examples of Semi-Stable and Unstable Bundles on the Quartic $K3$

We have previously seen in Subsection 3.4 the behavior of a slope-stable bundle under the generalized algorithm. For the stable bundle defined in (3.17), the algorithm

produces convergence to an Hermitian Yang-Mills solution of the form (4.6). The integrated error measure τ_{k_H} was shown to converge to zero in Figure 9. We now perform a simple experiment to see what happens when we apply the generalized Donaldson algorithm in a case where Theorem 4 does not apply, that is, for a non-stable bundle.

4.3.1 A Semi-Stable Bundle

First, let us explore the behavior of a properly semi-stable $SU(n)$ bundle. Such a bundle is not a solution to the Hermitian Yang-Mills equations, but can come arbitrarily close to a solution as we vary the bundle moduli. To illustrate this, consider a rank 3 bundle over the same Quartic $K3$, (3.16). We choose the $SU(3)$ monad bundle

$$0 \longrightarrow \mathcal{O}(-4) \xrightarrow{f_{\text{semi-stable}}} \mathcal{O}(-2) \oplus \mathcal{O}(-1)^{\oplus 2} \oplus \mathcal{O} \longrightarrow \mathcal{V}_{\text{semi-stable}} \longrightarrow 0 \ , \tag{4.9}$$

where

$$f_{\text{semi-stable}} = \begin{pmatrix} 3uz{+}2xz{+}7yz \\ (6u^2x{+}20u^2y{+}15uxy{+}5x^2y{+}3uy^2{+}10xy^2{+}18u^2z{+}21uxz \\ \qquad +7x^2z{+}6uyz{+}7xyz{+}7y^2z{+}8uz^2{+}16xz^2{+}10z^3) \\ 7u^2x{+}10uxy{+}4y^3{+}6uxz{+}5uyz{+}7uz^2{+}2xz^2{+}10yz^2{+}z^3 \\ 8u^4{+}6u^2yz{+}5uy^2z{+}5uyz^2{+}19xyz^2{+}7uz^3 \end{pmatrix} \tag{4.10}$$

and x, y, z, u are the homogeneous coordinates on $\mathbb{P}^3$. Here the map, $f_{\text{semi-stable}}$ is an element of $H^0(X, Hom(A, B))$, where $A = \mathcal{O}(-4)$ and $B = \mathcal{O} \oplus \mathcal{O}(-2) \oplus \mathcal{O}(-1)^{\oplus 2}$. The global sections of $\mathcal{V}_{\text{semi-stable}}$ can be computed as in (3.19) and (3.20).

The Harder-Narasimhan filtration of this bundle takes the simple form

$$\mathcal{O} \oplus \mathcal{F} \ , \tag{4.11}$$

where $\mathcal{F}$ is a rank 2 bundle with $c_1(\mathcal{F}) = 0$ defined by

$$0 \to \mathcal{O}(-4) \to \mathcal{O}(-2) \oplus \mathcal{O}(-1)^{\oplus 2} \to \mathcal{F} \to 0 \ . \tag{4.12}$$

This is an $SU(2)$ bundle, but it cannot solve the slope-zero Hermitian Yang-Mills equations. Instead, as described in point 2 above, for a generic value of the bundle moduli (4.10) we expect τ_{k_H} to converge to a constant, finite, positive number.

4.3.2 An Unstable Bundle with a Filtration by Line Bundles

As our next case, consider an unstable vector bundle with a Harder-Narasimhan filtration that is a sum of line bundles. We select a simple example for which $\mathcal{V}_{\text{unstable}}$ itself is the following sum of line bundles over the $K3$ in (3.16),

$$\mathcal{V}_{unstable\ sum} = \mathcal{O}(1) \oplus \mathcal{O}(-1) \ . \tag{4.13}$$

Here $\mathcal{V}$ is manifestly slope-unstable since $\mu(\mathcal{O}(1)) > \mu(\mathcal{V}_{unstable\ sum})$. From point $3(a)$ above, we expect the color matrix to take the form

$$g^{i\bar{j}}F_{i\bar{j}} \sim \begin{pmatrix} 1 & \\ & -1 \end{pmatrix} . \tag{4.14}$$

This form is the same globally, since the bundle is a direct sum. As a result, because error measure τ_{k_H} in (3.25) contains the sum of the absolute values of the eigenvalues of the color matrix, we expect that as $k_H \to \infty$ error measure $\tau_{k_H} \sim |\lambda_1| + |\lambda_2| \to 2$.

4.3.3 An Unstable Bundle with Sheaf Filtration

Next, consider the case of an unstable bundle with a more complicated Harder-Narasimhan filtration. On the Quartic $K3$ given by (3.16), we define the unstable $SU(2)$ monad bundle $\mathcal{V}_{\text{unstable}}$ by

$$0 \longrightarrow \mathcal{O}(-3) \xrightarrow{f} \mathcal{O}(1) \oplus \mathcal{O}(-2)^{\oplus 2} \longrightarrow \mathcal{V}_{\text{unstable}} \longrightarrow 0 , \tag{4.15}$$

where

$$f = (x_0^3x_2+5x_1x_2^3+10x_0^2x_1^2+7x_2x_1^3+4x_0x_3^3, x_1+15x_2+6x_3, 2x_0+x_2+3x_1+12x_3) \tag{4.16}$$

A simple analysis along the lines of [52] (see, for example, Hoppe's Criterion), reveals that $\mathcal{V}_{\text{unstable}}$ is a slope-unstable bundle. It is de-stabilized by a rank 1 sheaf, $\mathcal{F}$. Furthermore, the Harder-Narasimhan filtration of $\mathcal{V}_{\text{unstable}}$ is given simply by

$$\mathcal{O}_X(-1) \oplus \mathcal{F} , \tag{4.17}$$

where $\mathcal{F}$ is a rank one sheaf described by

$$0 \longrightarrow \mathcal{F} \longrightarrow \mathcal{O}(2)^{\oplus 2} \xrightarrow{g} \mathcal{O}(3) \longrightarrow 0 \tag{4.18}$$

with $\mathcal{F} = ker(g)$ and $c_1(\mathcal{F}) = 1$. This rank 1 object is a sheaf and not a line bundle because its rank can jump (from rank 1 to rank 2) over a higher co-dimensional locus in the base X. This occurs when the defining polynomial map, $g = (x_1 + \ldots, 2x_0 + \ldots)$ shares common zeros with the defining polynomial of the $K3$ surface in (2.22). It should be noted that $\mathcal{V}_{\text{unstable}}$ itself has no such singularities. It is a vector bundle, despite the presence of subsheaves such as $\mathcal{F}$ in (4.18). As a result, we expect the connection to produce a color matrix of the type shown in (4.8); that is,

$$g^{i\bar{j}}F_{i\bar{j}} \sim \begin{pmatrix} \mu_1(x) & \\ & -\mu_1(x) \end{pmatrix} . \tag{4.19}$$

Listed above are possible expected forms for the color matrix of several non-stable bundles. We now ask: what will the Donaldson algorithm produce when applied to

these examples? What behaviour do we expect for the error measure τ_{k_H}? How will the presence of filtration-sheaves, such as (4.17), manifest itself? Before we investigate these questions, it should be noted that the Harder-Narasimhan filtration of $\mathcal{V}_{\text{unstable}}$ is *almost* the same as the form of the previous example in (4.13). That is, the rank 1 sheaf $\mathcal{F}$ nearly everywhere resembles the line bundle $\mathcal{O}(1)$ except at points. As mentioned above, had this been the case there would be a clear prediction for the results of the integrated error measure. But what happens for $\mathcal{V}_{\text{unstable}}$ as defined in (4.15)? We turn now to an examination of the color matrix eigenvalues.

We present the numerical results for the three bundles above, as well as for the stable bundle (3.17) from Subsection 3.4. The error measure τ_{k_H} is plotted for these bundles in Figure 10. Despite the fact that these bundles are not solutions to the Hermitian Yang-Mills equations, we find that the way in which they fail to provide a solution are in exact agreement with the mathematical structure of semi-stable and unstable bundles. As expected from the Harder-Narasimhan filtrations, the three cases shown in Figure 10 can be distinguished by the behavior

$$\tau \sim \int \sum |\lambda_i| \longrightarrow \begin{cases} 0 & \text{(stable)} \\ \text{const.} > 0 & \text{(semi-stable)} \\ \text{const.} > 0 \text{ or } \infty & \text{(unstable)} \end{cases} \tag{4.20}$$

The error measure associated wth the semi-stable bundle $\mathcal{V}_{\text{semi-stable}}$ converges to a non-zero constant value. Furthermore, the unstable sum of line bundles produces a constant value $\tau_{k_H} = 2$. Somewhat surprisingly, we find that the error measure for $\mathcal{V}_{\text{unstable}}$ converges to a constant value of ~ 2, as if its Harder-Narasimhan filtration had been $\mathcal{O}(-1) \oplus \mathcal{O}(+1)$ (that is, of the $\mu = const.$ type described in (4.7)) instead of the actual filtration in (4.17). To understand the result for this last unstable bundle, one must look in more detail at the computation of the field strength and the behavior of the subsheaf $\mathcal{F}$ in the algorithm approximating the connection. This will be explored in detail in the next subsection. We will give an explicit discussion of how the T-operator fails to converge in this case, and how the generalized Donaldson algorithm none-the-less produces a connection that exhibits the correct physical singularities.

4.4 Eigenvalues Along a Geodesic

In this subsection, we explore in detail the behavior of the unstable bundle $\mathcal{V}_{\text{unstable}}$ on the Quartic $K3$. As discussed above, while the rank of $\mathcal{V}_{\text{unstable}}$ remains constant everywhere on the $K3$ surface X, the rank of a de-stabilizing subsheaf $\mathcal{F}$ in (4.18) can increase over a higher co-dimension locus in the base.

For the sheaf $\mathcal{F}$, one can find this singular locus by determining where the defining map g in (4.18) goes to zero over the Calabi-Yau (2.22). In this case, there are 4 point-like "instantons", that is, points in the base for which $\mathcal{F}$ jumps in rank. Such

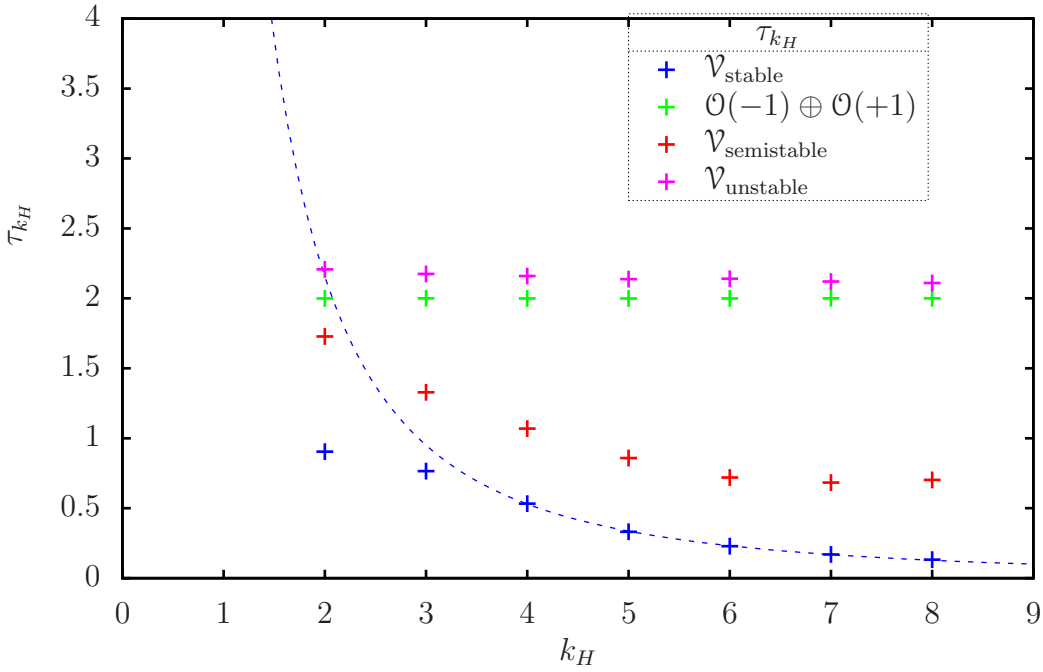

Figure 10: *The integrated error, τ_{k_H}, for $SU(n)$ bundles on the Quartic $K3$, (2.22). Shown above are the results for 1) the stable $SU(2)$ bundle $\mathcal{V}_{stable}$ defined in (3.17), 2) the semi-stable $SU(3)$ bundle $\mathcal{V}_{semi\text{-}stable}$ defined in (4.9), 3) the simple unstable sum of line bundles $\mathcal{O}(-1)\oplus \mathcal{O}(-1)$ and 4) the unstable $SU(2)$ bundle $\mathcal{V}_{unstable}$ defined in (4.15) with a Harder-Narasimhan filtration exhibiting sheaf singularities.*

instantons are described non-perturbatively in heterotic M-theory by a dissolved $M5$-brane on the $K3$ surface [63, 64]. In homogeneous coordinates, these points[3] are

$$\begin{aligned} p_0 &= \big[1 : -3.2279 - 1.6903i : -0.7510 - 2.6031i : 1.3874 + 2.8736i\big], \\ p_1 &= \big[1 : -3.2279 + 1.6903i : -0.7510 + 2.6031i : 1.3874 - 2.8736i\big], \\ p_2 &= \big[1 : -1.6951 - 0.3844i : 1.6095 - 0.5912i : -1.2183 + 0.6535i\big], \\ p_3 &= \big[1 : -1.6951 + 0.3844i : 1.6095 + 0.5920i : -1.2183 - 0.6535i\big]. \end{aligned} \tag{4.21}$$

To explore the behavior of the connection around, say, p_0, we chose a geodesic $P(s)$ that passes through this point. The approximate Calabi-Yau metric used for the geodesic was computed at $k_g = 15$, and the parameter s is normalized such that it coincides with the path length.

The geodesic is a solution of the differential equation

$$\frac{\partial^2 P^\lambda(s)}{\partial s^2} + \Gamma^\lambda_{\mu\nu} \frac{\partial P^\mu(s)}{\partial s} \frac{\partial P^\nu(s)}{\partial s} = 0 \ . \tag{4.22}$$

On a Kähler manifold, parallel transport does not mix holomorphic and anti-holomorphic coordinates. In other words, the Christoffel symbol

$$\Gamma^i_{jk} = g^{i\bar{h}} \partial_j g_{k\bar{h}} \tag{4.23}$$

has no mixed-index components. Therefore, the equation for the geodesic simplifies to

$$\frac{\partial^2 P^i(s)}{\partial s^2} + \Gamma^i_{jk} \frac{\partial P^j(s)}{\partial s} \frac{\partial P^k(s)}{\partial s} = 0 \ . \tag{4.24}$$

We normalize the initial velocity vector as

$$1 = g_{i\bar{j}} \frac{\partial P^i(s)}{\partial s} \overline{\frac{\partial P^j(s)}{\partial s}} \Big|_{s=0} \ , \tag{4.25}$$

so that the geodesic parameter s equals the metric path length. To numerically solve for $P(s)$, we used Newton's method with a step size of 10^{-3}. After each integration step, we projected back onto the K3 hypersurface. Some sample points along our chosen geodesic are

$$\begin{aligned} P(0) &= p_0, \\ P(0.05) &= \big[1.005 + 0.001i : -3.228 - 1.690i : -0.749 - 2.593i : 1.387 + 2.879i\big], \\ P(1) &= \big[1.640 + 0.372i : -3.228 - 1.690i : -0.426 - 0.058i : 1.117 + 3.389i\big], \\ P(2) &= \big[2.127 + 0.968i : -3.228 - 1.690i : -0.528 + 2.744i : 0.608 + 3.501i\big]. \end{aligned} \tag{4.26}$$

[3]Such degeneracies can be easily found using computational algebraic geometry packages such as [65, 66, 67].

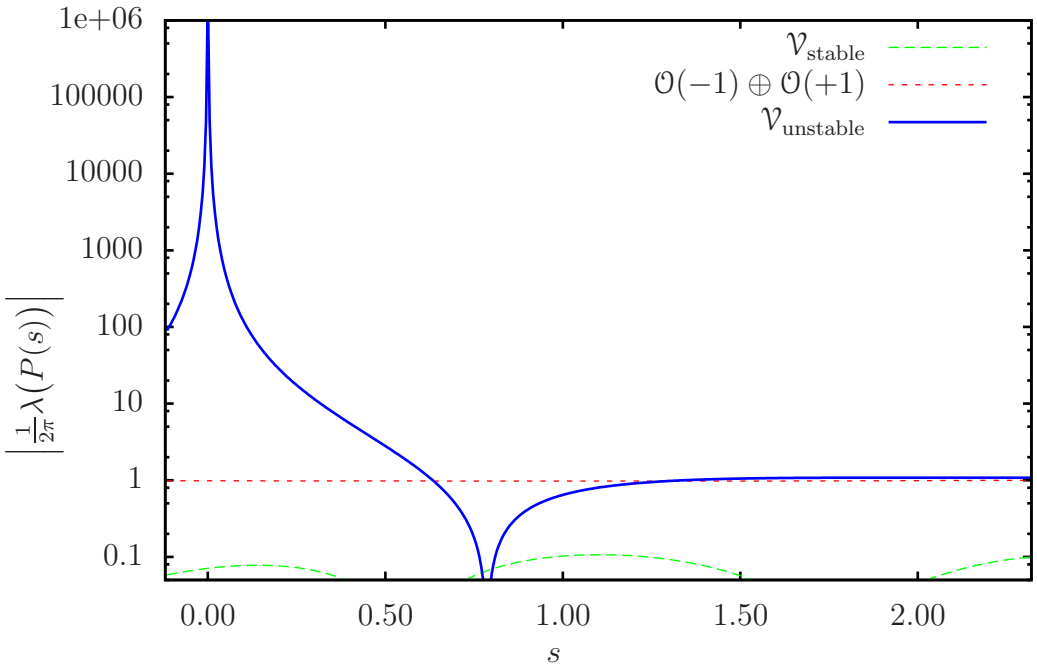

Figure 11: *The eigenvalues of $g^{i\bar{j}}F_{i\bar{j}}$ along the geodesic $P(s)$. The indecomposable, unstable bundle $\mathcal{V}_{unstable}$ is the thick blue line, and one of its point-like instantons is located at $s = 0$. For comparison, the eigenvalues for the balanced connection on the sum of line bundles* (4.13) *are given by the red line, while that for the stable bundle* (3.17) *is shown by the green line.*

We now compute $g^{i\bar{j}}F_{i\bar{j}}$ for $\mathcal{V}_{\text{unstable}}$ at each point of the geodesic. Recall that $\mathcal{V}_{\text{unstable}}$ remains a bundle everywhere. We want to know: what happens to the color matrix $g^{i\bar{j}}F_{i\bar{j}}$ near the $\mathcal{F}$-sheaf singular point $P(0)$? Since the vector bundles we are considering here are of rank 2, there are two real eigenvalues. After untwisting with the determinant line bundle, they are $\pm\lambda\big(P(s)\big)$. We plot these eigenvalues in Figure 11. Note, since $\mathcal{V}_{\text{unstable}}$ is an $SU(2)$ bundle, the two eigenvalues are λ and $-\lambda$. We plot only the positive eigenvalue. For comparison, we also compute the color matrix for the sum of line bundles $\mathcal{O}(-1)\oplus\mathcal{O}(+1)$ and the stable bundle, $\mathcal{V}_{\text{stable}}$ from (3.17) along the same geodesic. Since we are interested in the accuracy of our numerical approximation to the slope-unstable connections, we list here the details of this preliminary calculation (in the sense that we have performed only a few iterations of the non-converging T-operator).

- The Calabi-Yau metric (which determines the Kähler form ω as wells as the geodesic P) was computed at degree $k_g = 15$.
- The metric T-operator was iterated 15 times, numerically integrating over 2,000,000 points.

- The Hermitian Yang-Mills connection $F_{i\bar{j}}$ was computed at degree $k_H = 7$.
- The connection T-operator was iterated 30 times, numerically integrating over 1,000,000 points.

By inspecting Figure 11, we see that the results for the stable bundle $\mathcal{V}_{\text{stable}}$ and the unstable sum of line bundles $\mathcal{O}(-1) \oplus \mathcal{O}(+1)$ behave smoothly along the geodesic. The eigenvalues for the stable bundle $\mathcal{V}_{\text{stable}}$ (green dashed line) are close to zero, as they should be for a slope-stable bundle with $c_1(\mathcal{V}_{\text{stable}}) = 0$. Likewise, the eigenvalues for the reducible bundle $\mathcal{O}(-1) \oplus \mathcal{O}(+1)$ are approximately constant and equal to the expected value

$$\frac{1}{2\pi}\lambda = c_1\big(\mathcal{O}(1)\big) = 1 \ . \tag{4.27}$$

More interestingly, as predicted, the eigenvalues for the unstable bundle $\mathcal{V}_{\text{unstable}}$ have a pole at $P(0)$, the location of the point-like instanton. Note that due to the log-scale in Figure 11, the width of this pole appears somewhat elongated. In reality, this divergence is very close to a δ-function, $\delta(s = 0)$. Away from that point, $\frac{1}{2\pi}\lambda \approx 1$. This eigenvalue was precisely the value that was obtained in Figure 10 by the general numerical integration (which did not include the points (4.21)).

As a final observation, note that the "dip" in the eigenvalues, where $\lambda \to 0$ before assuming the constant value, is a function of the fact that the bundle $\mathcal{V}_{\text{unstable}}$ is not defined globally as a direct sum. That is, near the singularity at $s = 0$ the eigenvalues of the color matrix have the form $\left(\begin{smallmatrix} \lambda & \\ & -\lambda \end{smallmatrix}\right)$, whereas sufficiently far from the singularity, for $s \gtrsim 0.9$, we find that the color matrix has "switched" the position of its positive and negative eigenvalues; that is, $\left(\begin{smallmatrix} -1 & \\ & 1 \end{smallmatrix}\right)$. In transitioning between these two configurations, the eigenvalues must go to zero. We conjecture that the failure of the eigenvalues to decompose globally into + and − values is in one-to-one correspondence with the fact that $\mathcal{V}_{\text{unstable}}$ is not defined as a direct sum of line bundles but, rather, as an indecomposable rank 2 bundle. There is no physical significance to the point where these eigenvalues approach zero. In fact, we will see in the next subsections that as one increases the accuracy of our computation (specifically, higher iterations of the T-operator and of the k_H-twisting) the position of this zero approaches the δ-function spike at $s = 0$.

4.4.1 Iterating the T-Operator

It is clear that the T-operator (3.6) on the matrices $H_{\alpha\bar{\beta}}$ does *not* converge for $\mathcal{V}_{\text{unstable}}$. As noted in Subsection 3.1, the T-operator converges if and only if the bundle is Gieseker stable and $\mathcal{V}_{\text{unstable}}$ is manifestly Gieseker unstable[4]. Indeed, since the T-

[4]To see that $\mathcal{V}_{\text{unstable}}$ is not Gieseker stable, note that from (3.7), $P_{\mathcal{O}(1)}(\mathcal{F})(n) = \chi(\mathcal{F} \otimes \mathcal{O}(n)) = 2n(2+n)$ while $P_{\mathcal{O}(1)}(\mathcal{V})(n) = \chi(\mathcal{V} \otimes \mathcal{O}(n)) = 2(1+n^2)$. Hence, for $n \gg 1$, $P_{\mathcal{O}(1)}(\mathcal{V}) \prec P_{\mathcal{O}(1)}(\mathcal{F})$ and $\mathcal{V}$ is Gieseker unstable.

operator has to reproduce the field-strength singularity at the location of the point-like instanton, some components of the $H_{\alpha\bar{\beta}}$ matrix must grow beyond bound as we approximate the balanced connection.

To see this behavior, consider higher iterations of the T-operator. We approximate the field strength $F_{i\bar{j}}$ at fixed degree $k_H = 5$, and compute the T-operator by numerically integrating using 500,000 points. The results of the first 20 iterations of the T-operater are plotted in Figure 12. Despite the fact that the T-operator is clearly failing to converge, and, hence, the results of Theorem 4 do not apply, the numerical evidence presented here strongly suggests that the balanced connection is still a well-defined limit as we continue iterating the T-operator.

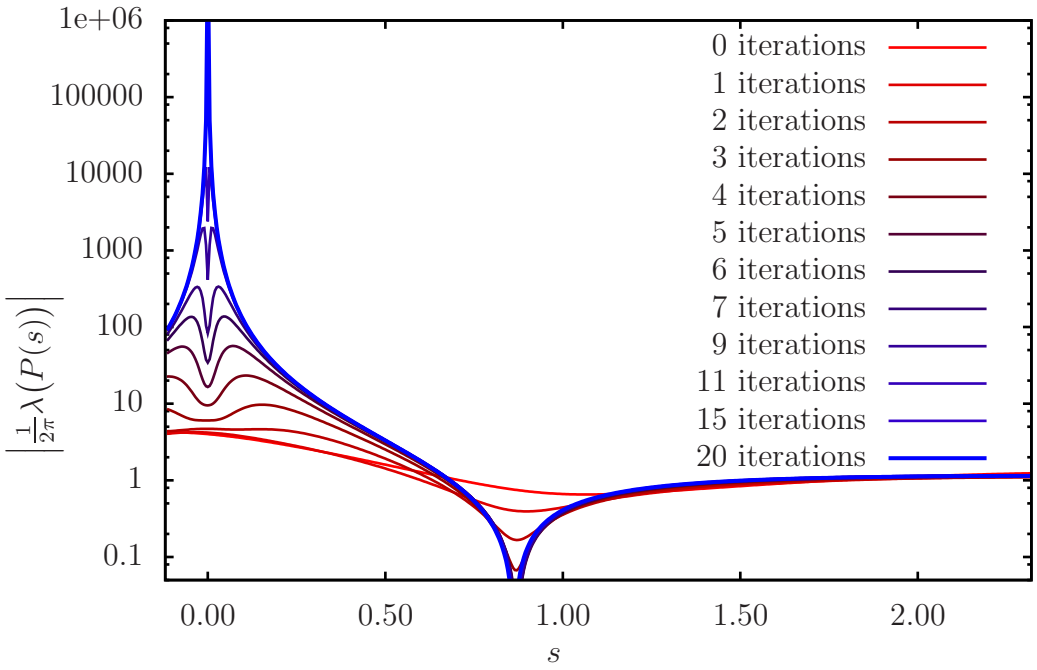

Figure 12: *The eigenvalues $\lambda\big(P(s)\big)$ of $g^{i\bar{j}}F_{i\bar{j}}$ along the geodesic $P(s)$. The point-like instanton is located at $s = 0$. The Hermitian Yang-Mills connection was approximated at degree $k_H = 5$, and the bundle T-operator was iterated between 0 and 20 times.*

As a final exploration of this behavior, we perform the computation of the connection at the limit of our accuracy, that is, for both a high degree of twisting and a large number of iterations of the T-operator.

4.4.2 Degree of Twisting

In this subsection, we compute the color matrix $g^{i\bar{j}}F_{i\bar{j}}$ at degrees ranging from $k_H = 2$ to $k_H = 8$. The connection T-operator was numerically integrated using 1,000,000 points. For small degrees k_H, some entries of $H_{\alpha\bar{\beta}}$ grow quickly at each iteration, and

the iteration must be stopped before the machine precision becomes insufficient. This is why we performed only 7 and 15 iterations at $k_H = 2$ and $k_H = 3$. For larger degrees $k_H \geq 4$, the matrix entries grow slowly enough that this is not an issue. The results are shown in Figure 13.

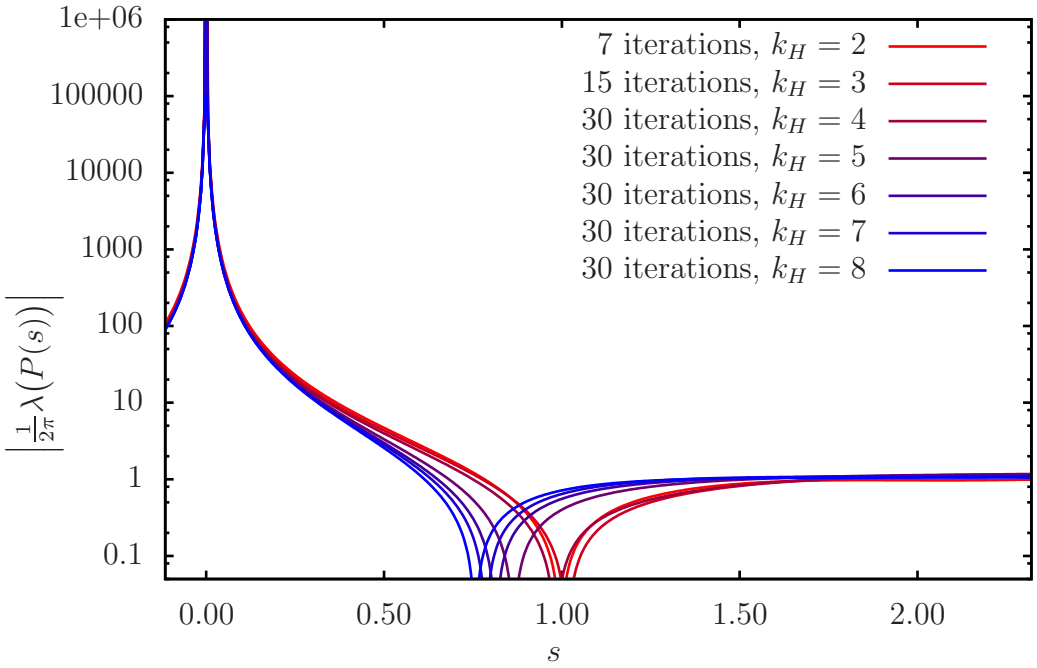

Figure 13: *The eigenvalues $\lambda\big(P(s)\big)$ of $g^{i\bar{j}}F_{i\bar{j}}$ along the geodesic $P(s)$. The point-like instanton is located at $s = 0$. The different lines correspond to different degrees k_H at which the Hermitian Yang-Mills connection was approximated. The divergent peak at $s = 0$ is approaching a δ-funtion $\delta(s = 0)$ as $k_H \to \infty$.*

For a bundle of the form $\mathcal{V}_{\text{unstable}}$ in (4.15), we conjecture that as $k_H \to \infty$ the color matrix can be decomposed as sum of a divergent piece (due to the sheaf $\mathcal{F}$ in (4.17) in its Harder-Narasimhan filtration) plus a constant eigenvalue contribution (due to the "smoothing" of its Harder-Narasimhan filtration to $\mathcal{O}(-1) \oplus \mathcal{O}(1)$ far from the points (4.21)). That is,

$$\text{(point-like instanton)} + \text{(constant } \lambda \text{ elsewhere)}. \tag{4.28}$$

This conjecture explains the convergence of τ_{k_H} to a constant value shown in Figure 10. Specifically, that

$$\lim_{k_H\to\infty} \tau_{k_H}\Big(\mathcal{V}_{\text{unstable}}\Big) = \lim_{k_H\to\infty} \tau_{k_H}\Big(\mathcal{O}(-1) \oplus \mathcal{O}(+1)\Big) = 2 \tag{4.29}$$

for regions away from the point-like instantons.

In summary, the results of the past few sections have given substantial evidence that even in the cases where a bundle $\mathcal{V}$ does not solve the Hermitian Yang-Mills equations (and, hence, the T-operator does not coverge), the generalized Donaldson algorithm still produces a physically relevant connection. In particular, in view of the results in Figure 13 it seems possible that even in the case of an unstable vector bundle for which the color matrix $g^{i\bar{j}}F_{i\bar{j}}$ diverges, the generalized Donaldson algorithm is providing an accurate approximation of the field strength $F_{i\bar{j}}$. In the limit as k_H increases, as well as the iterations of the T-operator, we find that while the T-operator is not converging, the resulting connection not only correctly displays the field strength singularities due the sub-sheaf singularities, but also the smooth asymptotic behavior away from any singular loci.

With these observations in hand, we conclude that it is possible to apply the generalized Donaldson algorithm to an arbitrary holomorphic vector bundle and to determine its slope-stability properties by inspection of the results, such as those shown in Figure 10. This observation provides a useful new tool for determining the existence of supersymmetric vacua in heterotic compactifications.

4.5 Rank Three Bundles on the Quintic

Having learned what behavior to expect from stable, semi-stable, and unstable bundles under the generalized Donaldson algorithm, we now present examples involving higher rank bundles on a Calabi-Yau threefold. This is the type of geometry that is ultimately of interest to us in $\mathcal{N} = 1$ supersymmetric heterotic compactifications.

Specifically, we consider the deformed Fermat Quintic, denoted $\mathbb{P}^4[5]$, defined by

$$u^5 + v^5 + x^5 + y^5 + z^5 + \tfrac{5}{2}uvxyz = 0 \ , \tag{4.30}$$

where u, v, x, y, z are the homogeneous coordinates of $\mathbb{P}^4$. As was the case on the Quartic $K3$, the Kähler cone of the Quintic is 1-dimensional and all line bundles $\mathcal{L}$ on X can be written as $\mathcal{O}(n)$ for some integer n. The global sections of $\mathcal{O}(n)$ on X can be defined as a polynomial space whose dimension is given by

$$h^0(X, \mathcal{O}(n)) = \begin{cases} 0 & n < 0 \\ \binom{n+4}{4} & 0 \leq n < 5 \\ \binom{n+4}{4} - \binom{n-1}{4} & n \geq 5 \end{cases} \ . \tag{4.31}$$

With these definitions in hand, one can compute a basis of polynomials of $H^0(X, \mathcal{V} \otimes \mathcal{L}^{k_H})$ of the degree given by (4.31).

As in previous sections, we will investigate three types of vector bundle that are respectively 1) stable, 2) semi-stable and 3) unstable. We will consider two different types of unstable bundles– one an indecomposable rank 3 bundle and the other an unstable sum of three line bundles. The monad bundles are defined as follows.

4.5.1 A stable bundle

The stable $SU(3)$ bundle $\mathcal{V}_{\text{stable}}$ is given by

$$0 \longrightarrow \mathcal{O}(-2)^{\oplus 3} \xrightarrow{f_{\text{stable}}} \mathcal{O}(-1)^{\oplus 6} \longrightarrow \mathcal{V}_{\text{stable}} \longrightarrow 0 \ , \tag{4.32}$$

where the monad map is defined (via a map on sections) as

$$f_{\text{stable}} = \begin{pmatrix} 5u{+}24v{+}3x{+}7y{+}18z & 11u{+}14v{+}18x{+}14y{+}29z & 12u{+}16v{+}11x{+}13y{+}16z \\ 9u{+}22v{+}12x{+}14y{+}3z & 8u{+}4x{+}9z & 20u{+}33v{+}9x{+}18y{+}34z \\ 6x{+}3y & 3u{+}v{+}2x{+}13y{+}18z & 24u{+}23v{+}46x{+}17y{+}38z \\ 10v{+}12y{+}10z & 6v{+}11x{+}9y & 36u{+}21v{+}12x{+}37y{+}28z \\ 13u{+}26v{+}18x{+}13y{+}12z & 5u{+}11v{+}6x{+}9y{+}12z & 3u{+}18x{+}15y{+}12z \\ 20u{+}28v{+}5x{+}12y{+}17z & 12u{+}14v{+}28x{+}6y{+}7z & 10u{+}4y{+}6z \end{pmatrix} \ . \tag{4.33}$$

As in the previous sections, since the Kähler cone of the Quintic is one-dimensional, it is straightforward to verify that $\mathcal{V}_{\text{stable}}$ is slope-stable by checking that $H^0(X, \wedge^k V) = 0$ for $k = 1, \ldots 2$ (Hoppe's criterion [54, 62]). Applying the generalized Donaldson algorithm to the computation of the connection on $\mathcal{V}_{\text{stable}}$, we find that the T-operator converges as expected and that the error measure, (3.25), converges smoothly to zero. The results are shown in Figure 14.

4.5.2 A semi-stable bundle

A semi-stable $SU(3)$ bundle is defined by the following short exact sequence

$$0 \longrightarrow \mathcal{O}(-3) \xrightarrow{f_{\text{semi-stable}}} \mathcal{O}(-1)^{\oplus 3} \oplus \mathcal{O} \longrightarrow \mathcal{V}_{\text{semi-stable}} \longrightarrow 0 \ , \tag{4.34}$$

where $f_{\text{semi-stable}}$ is

$$f_{\text{semi-stable}} = \begin{pmatrix} 4u^2{+}uv{+}11ux{+}15vx{+}8x^2{+}15vy{+}xy{+}16uz{+}21vz{+}26xz{+}14yz{+}36z^2 \\ 5u^2{+}4uv{+}19ux{+}9vx{+}8uy{+}6vy{+}10xy{+}y^2{+}24uz{+}21vz{+}17xz{+}9yz \\ (2u^2{+}6uv{+}20vv{+}15ux{+}5vx{+}14uy{+}12vy{+}19xy{+}5vz{+}4z^2) \\ (4u^3{+}10u^2v{+}13uvx{+}15uvy{+}uxy{+}16vxy{+}uy^2{+}5xy^2{+}5y^3 \\ {+}6u^2z{+}3uvz{+}6v^2z{+}7uxz{+}11vxz{+}9uyz{+}8vyz{+}9xyz{+}5y^2z{+}8vz^2{+}6xz^2{+}4yz^2) \end{pmatrix} \ . \tag{4.35}$$

In this case, the bundle admits a subsheaf, $\mathcal{O} \subset \mathcal{V}_{\text{semi-stable}}$ with $\mu(\mathcal{O}) = \mu(\mathcal{V}_{\text{semi-stable}})$. Hence, $\mathcal{V}_{\text{semi-stable}}$ is properly semi-stable, not polystable, and will not admit a solution to the Hermitian Yang-Mills equations. Its Jordan-Hölder filtration (4.5) is given simply by

$$\mathcal{F} \oplus \mathcal{O} \ , \tag{4.36}$$

where the rank 2 sheaf $\mathcal{F}$ is defined by

$$0 \to \mathcal{F} \to \mathcal{O}(1)^{\oplus 3} \to \mathcal{O}(3) \to 0 \ . \tag{4.37}$$

Because the S-equivalence class containing $\mathcal{V}_{\text{semi-stable}}$ contains a poly-stable representative, this semi-stable bundle may be brought arbitrarily close to a solution of the Hermitian Yang-Mills equations by varying the bundle moduli (that is, bringing $\mathcal{V}_{\text{semi-stable}}$ closer to the direct sum bundle, (4.36)).

4.5.3 Unstable bundles

As in previous sections, we will compare the behavior of two unstable bundles.

1. **An unstable direct sum:**

   First, consider the simple unstable direct sum defined by

   $$\mathcal{V}_{sum} = \mathcal{O}(-1) \oplus \mathcal{O}(-1) \oplus \mathcal{O}(2) \quad . \tag{4.38}$$

   $\mathcal{V}_{sum}$ is a direct sum of stable objects, but because the three line bundles do not have the same slope, the sum is unstable. As in (4.7), the color matrix is given by

   $$g^{i\bar{j}} F_{i\bar{j}} = \begin{pmatrix} -1 & & \\ & -1 & \\ & & 2 \end{pmatrix} \quad . \tag{4.39}$$

   The error measure, (3.25), is predicted to lie at $\tau_{k_H} = 4$.

2. **An indecomposable unstable bundle:**

   We can define an unstable $SU(3)$ bundle as follows,

   $$0 \longrightarrow \mathcal{O}(-2) \xrightarrow{f_{\text{unstable}}} \mathcal{O}(-1)^{\oplus 4} \oplus \mathcal{O}(1) \longrightarrow \mathcal{V}_{\text{unstable}} \longrightarrow 0 \tag{4.40}$$

   with

   $$f_{\text{unstable}} = \begin{pmatrix} x+6y+18z \\ 13u+11x+9y \\ 7u+11v+4z \\ (4u^3+10u^2v+13uvx+15uvy+uxy+16vxy+uy^2+5xy^2+5y^3+6u^2z+3uvz \\ +6v^2z+7uxz+11vxz+9uyz+8vyz+9xyz+5y^2z+8vz^2+6xz^2+4yz^2) \end{pmatrix} \quad . \tag{4.41}$$

   Here $\mathcal{V}_{\text{unstable}}$ is destabilized by the sub-bundle $\mathcal{O}(1)$ with $\mu(\mathcal{O}(1)) > 0$. The graded sum, (4.5), associated with its Harder-Narasimhan filtration is given simply by

   $$\mathcal{G} \oplus \mathcal{O}(1) \ , \tag{4.42}$$

   where $\mathcal{G}$ is a rank 3 sheaf with $c_1(\mathcal{G}) = -1$ defined by

   $$0 \to \mathcal{O}(-2) \to \mathcal{O}(-1)^{\oplus 3} \to \mathcal{G} \to 0 \quad . \tag{4.43}$$

   As discussed in Subsections 4.3 and 4.4, we would not expect that since $|c_1(\mathcal{G})| = |c_1(\mathcal{O}(1))| = 1$, the error measure should approximate $\tau_{k_H} = 2$.

In these calculations, the metric on the Quintic threefold was computed at degree $k_g = 8$, the metric T-operator was iterated 10 times and the numerical integration was carried out with 2,000,000 points. In addition, the connection T-operator was iterated 10 times, the numerical integration used 1,000,000 points and the τ_{k_H} integral was computed numerically with 100,000 points.

The comparison between the stable, (4.32), semi-stable, (4.34), and the two unstable bundles, (4.38) and (4.40), is given in Figure 15.

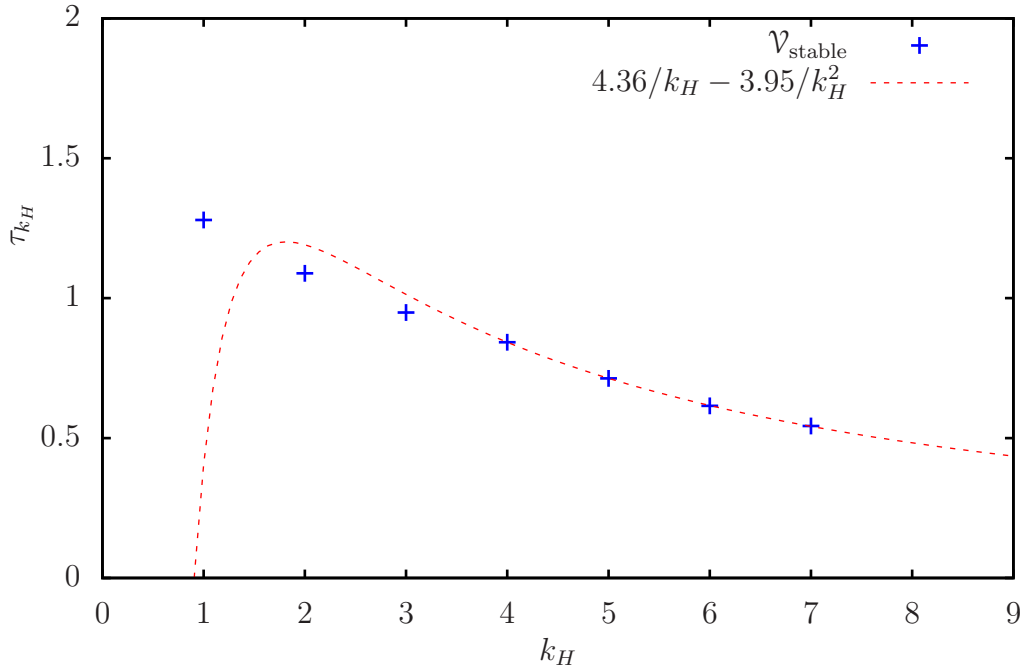

Figure 14: *The integrated error measure τ_{k_H} on the Quintic threefold for the stable bundle defined in* (4.32).

5 Conclusions and future work

Donaldson's algorithm [38, 39, 40] has been shown to be an important tool in the computation of Ricci-flat metrics on Calabi-Yau manifolds. Numerical implementations of this algorithm were given in [48, 49, 50, 43] and a generalization of these techniques to Hermitian metrics on holomorphic vector bundles was proposed in [42, 43]. In this paper, we have presented a systematic and efficient method to implement the generalized Donaldson algorithm and to numerically compute Hermitian Yang-Mills connections satisfying (1.1). We illustrated this by, first, computing the Ricci-flat Calabi-Yau metrics on the Quartic $K3$ surface and the Quintic threefold and, second, over these manifolds, calculating the Hermitian Yang-Mills connection on several holomorphic vector bundles defined via the monad construction [51, 52, 53, 25].

In addition to showing that the algorithm converges to the Hermitian Yang-Mills connection for a slope-stable bundle, we presented results demonstrating that even in the case of unstable vector bundles, for which the generalized T-operator (3.6) does not converge, the algorithm produces a physically relevant connection. In Section 4, we showed that the connection produced by the generalized Donaldson algorithm in the case of an unstable bundle can be understood in terms of the Harder-Narasimhan filtration [54] of an unstable sheaf by semi-stable subsheaves. Furthermore, as shown in Subsection 4.4, in cases where the filtrations contain sheaves with curvature singularities, the presence of such singularities can be accurately described by the algorithm.

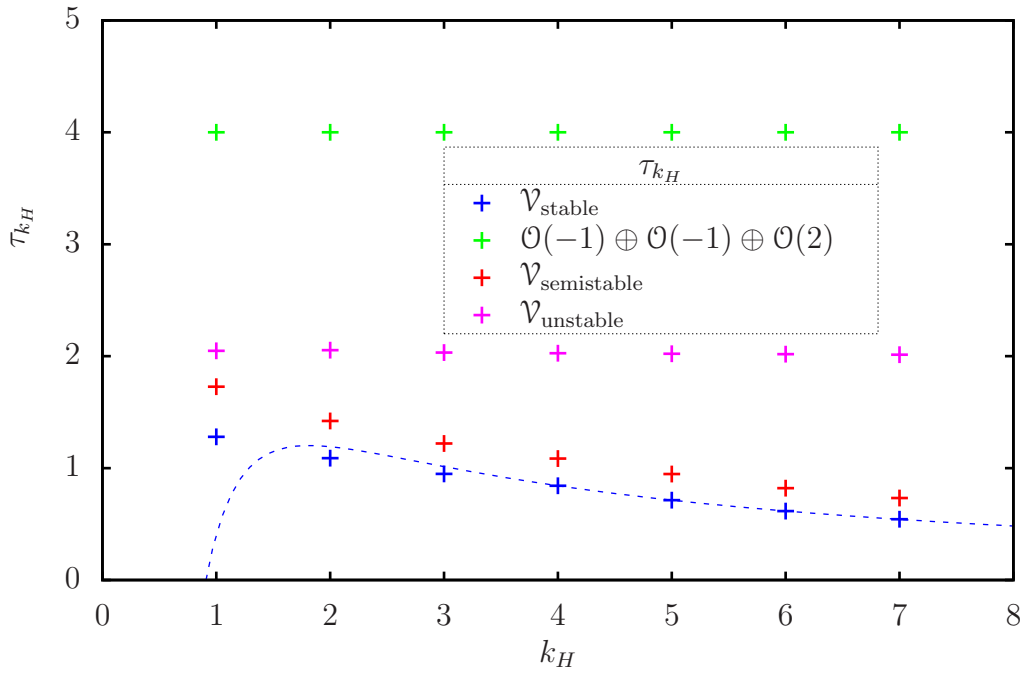

Figure 15: *Comparison of different bundles on the Quintic threefold. The stable bundle,* (4.32)*, exhibits the behavior of a Hermitian Yang-Mills connection and the error τ_{k_H} decreases as the degree k_H is increased. Meanwhile, the unstable,* (4.40)*, and strictly semi-stable,* (4.34)*, bundles approach a fixed, non-zero constant value. The results for the semi-stable bundle depend on the choice of bundle moduli and can be made to converge to a constant arbitrarily close to zero.*

These results may shed light on the mathematical study of non-Hermitian Yang-Mills connections [68].

Importantly, our results for unstable bundles allow us to apply the generalized Donaldson algorithm to arbitrary vector bundles arising in heterotic string compactifications and use it to determine whether such geometries admit supersymmetric vacua. The problem of deciding whether or not a given holomorphic vector bundle is slope-stable is a notoriously difficult one. Particularly challenging is the fact that the difficulty of a stability analysis generally increases rapidly with the dimension, $h^{1,1}$, of the Kähler cone. One of the great advantages of the algorithm presented in this paper is that, unlike in a standard analytic analysis, such numerical calculations can, in principle, be performed with essentially equal ease in arbitrary $h^{1,1}$ dimensions, thereby providing an important new tool in the analysis of supersymmetric heterotic vacua.

In recent work, [56, 57], the dependence of the slope-stability property of a vector bundle on the Kähler and bundle moduli has been explored from the point of view of four-dimensional effective field theory. The presence of "stability walls" separating stable and unstable regions of Kähler moduli space has been shown to have a variety of interesting physical and mathematical consequences [58, 69]. In future work [70], we will use the numerical techniques presented here to further explore the moduli dependence of supersymmetric solutions.

Finally, it is worth noting that the results of this paper are an important step forward in the computation of observable quantities of particle physics, such as the matter-field Kähler potential and physical Yukawa couplings. We hope to explore these applications in the future.

Acknowledgments

The work of L. Anderson and B. A. Ovrut is supported in part by the DOE under contract No. DE-AC02- 76-ER-03071 and by NSF RTG Grant DMS-0636606. L. Anderson, V. Braun and B. Ovrut would like to thank the Kavli Institute for Theoretical Physics for hospitality while this work was being completed.

Bibliography

[1] D. J. Gross, J. A. Harvey, E. J. Martinec, and R. Rohm, "The Heterotic String," *Phys. Rev. Lett.* **54** (1985) 502–505.

[2] P. Candelas, G. T. Horowitz, A. Strominger, and E. Witten, "Vacuum Configurations for Superstrings," *Nucl. Phys.* **B258** (1985) 46–74.

[3] P. Horava and E. Witten, "Heterotic and type I string dynamics from eleven dimensions," *Nucl. Phys.* **B460** (1996) 506–524, hep-th/9510209.

[4] P. Horava and E. Witten, "Eleven-Dimensional Supergravity on a Manifold with Boundary," *Nucl. Phys.* **B475** (1996) 94–114, hep-th/9603142.

[5] E. Witten, "Strong Coupling Expansion Of Calabi-Yau Compactification," *Nucl. Phys.* **B471** (1996) 135–158, hep-th/9602070.

[6] R. Friedman, J. Morgan, and E. Witten, "Vector bundles and F theory," *Commun. Math. Phys.* **187** (1997) 679–743, hep-th/9701162.

[7] R. Y. Donagi, "Principal bundles on elliptic fibrations," in *eprint arXiv:alg-geom/9702002*, pp. 2002–+. Feb., 1997.

[8] A. Lukas, B. A. Ovrut, and D. Waldram, "Non-standard embedding and five-branes in heterotic M- theory," *Phys. Rev.* **D59** (1999) 106005, hep-th/9808101.

[9] R. Donagi, B. A. Ovrut, T. Pantev, and D. Waldram, "Standard-model bundles," *Adv. Theor. Math. Phys.* **5** (2002) 563–615, math/0008010.

[10] R. Donagi, A. Lukas, B. A. Ovrut, and D. Waldram, "Holomorphic vector bundles and non-perturbative vacua in M- theory," *JHEP* **06** (1999) 034, hep-th/9901009.

[11] R. Blumenhagen, S. Moster, and T. Weigand, "Heterotic GUT and Standard Model vacua from simply connected Calabi-Yau manifolds," hep-th/0603015.

[12] R. Blumenhagen, S. Moster, R. Reinbacher, and T. Weigand, "Massless spectra of three generation U(N) heterotic string vacua," *JHEP* **05** (2007) 041, hep-th/0612039.

[13] A. Lukas, B. A. Ovrut, and D. Waldram, "On the four-dimensional effective action of strongly coupled heterotic string theory," *Nucl. Phys.* **B532** (1998) 43–82, hep-th/9710208.

[14] A. Lukas, B. A. Ovrut, K. S. Stelle, and D. Waldram, "The universe as a domain wall," *Phys. Rev.* **D59** (1999) 086001, hep-th/9803235.

[15] A. Lukas, B. A. Ovrut, K. S. Stelle, and D. Waldram, "Heterotic M-theory in five dimensions," *Nucl. Phys.* **B552** (1999) 246–290, hep-th/9806051.

[16] R. Donagi, B. A. Ovrut, T. Pantev, and D. Waldram, "Standard models from heterotic M-theory," *Adv. Theor. Math. Phys.* **5** (2002) 93–137, hep-th/9912208.

[17] R. Y. Donagi, J. Khoury, B. A. Ovrut, P. J. Steinhardt, and N. Turok, "Visible branes with negative tension in heterotic M- theory," *JHEP* **11** (2001) 041, hep-th/0105199.

[18] R. Donagi, Y.-H. He, B. A. Ovrut, and R. Reinbacher, "Moduli dependent spectra of heterotic compactifications," *Phys. Lett.* **B598** (2004) 279–284, hep-th/0403291.

[19] V. Braun, B. A. Ovrut, T. Pantev, and R. Reinbacher, "Elliptic Calabi-Yau threefolds with Z(3) x Z(3) Wilson lines," *JHEP* **12** (2004) 062, hep-th/0410055.

[20] R. Donagi, Y.-H. He, B. A. Ovrut, and R. Reinbacher, "The spectra of heterotic standard model vacua," *JHEP* **06** (2005) 070, hep-th/0411156.

[21] V. Braun, Y.-H. He, B. A. Ovrut, and T. Pantev, "A heterotic standard model," *Phys. Lett.* **B618** (2005) 252–258, hep-th/0501070.

[22] V. Braun, Y.-H. He, B. A. Ovrut, and T. Pantev, "Vector bundle extensions, sheaf cohomology, and the heterotic standard model," *Adv. Theor. Math. Phys.* **10** (2006) 4, hep-th/0505041.

[23] V. Braun, Y.-H. He, B. A. Ovrut, and T. Pantev, "The exact MSSM spectrum from string theory," *JHEP* **05** (2006) 043, hep-th/0512177.

[24] V. Bouchard and R. Donagi, "An SU(5) heterotic standard model," *Phys. Lett.* **B633** (2006) 783–791, hep-th/0512149.

[25] L. B. Anderson, J. Gray, Y.-H. He, and A. Lukas, "Exploring Positive Monad Bundles And A New Heterotic Standard Model," *JHEP* **02** (2010) 054, 0911.1569.

[26] M. Ambroso and B. A. Ovrut, "The B-L/Electroweak Hierarchy in Smooth Heterotic Compactifications," 0910.1129.

[27] M. Ambroso and B. Ovrut, "The B-L/Electroweak Hierarchy in Heterotic String and M- Theory," *JHEP* **10** (2009) 011, 0904.4509.

[28] P. Candelas and S. Kalara, "Yukawa couplings for a three generation superstring compactification," *Nucl. Phys.* **B298** (1988) 357.

[29] P. Candelas, X. C. De La Ossa, P. S. Green, and L. Parkes, "A pair of Calabi-Yau manifolds as an exactly soluble superconformal theory," *Nucl. Phys.* **B359** (1991) 21–74.

[30] B. R. Greene, D. R. Morrison, and M. R. Plesser, "Mirror manifolds in higher dimension," *Commun. Math. Phys.* **173** (1995) 559–598, `hep-th/9402119`.

[31] V. Braun, Y.-H. He, and B. A. Ovrut, "Yukawa couplings in heterotic standard models," *JHEP* **04** (2006) 019, `hep-th/0601204`.

[32] R. Donagi, R. Reinbacher, and S.-T. Yau, "Yukawa couplings on quintic threefolds," `hep-th/0605203`.

[33] L. B. Anderson, J. Gray, D. Grayson, Y.-H. He, and A. Lukas, "Yukawa Couplings in Heterotic Compactification," `0904.2186`.

[34] M. B. Green, J. H. Schwarz, and E. Witten, "SUPERSTRING THEORY. VOL. 1: INTRODUCTION,". Cambridge, Uk: Univ. Pr. (1987) 469 P. (Cambridge Monographs On Mathematical Physics).

[35] S. T. Yau, "On the Ricci curvature of a compact Kähler manifold and the complex Monge-Ampère equation. I," *Comm. Pure Appl. Math.* **31** (1978), no. 3, 339–411.

[36] K. Uhlenbeck and S.-T. Yau., "On the existence of Hermitian Yang-Mills connections in stable bundles," *Comm. Pure App. Math.* **39** (1986) 257.

[37] S. Donaldson, "Anti Self-Dual Yang-Mills Connections over Complex Algebraic Surfaces and Stable Vector Bundles,," *Proc. London Math. Soc.* **3** (1985) 1.

[38] S. K. Donaldson, "Scalar curvature and projective embeddings. II," *Q. J. Math.* **56** (2005), no. 3, 345–356.

[39] S. K. Donaldson, "Scalar curvature and projective embeddings. I," *J. Differential Geom.* **59** (2001), no. 3, 479–522.

[40] S. K. Donaldson, "Some numerical results in complex differential geometry," `math.DG/0512625`.

[41] G. Tian, "On a set of polarized Kähler metrics on algebraic manifolds," *J. Differential Geom.* **32** (1990), no. 1, 99–130.

[42] X. Wang, "Canonical metrics on stable vector bundles," *Comm. Anal. Geom.* **13** (2005), no. 2, 253–285.

[43] M. R. Douglas, R. L. Karp, S. Lukic, and R. Reinbacher, "Numerical solution to the hermitian Yang-Mills equation on the Fermat quintic," `hep-th/0606261`.

[44] M. Headrick and T. Wiseman, "Numerical Ricci-flat metrics on $K3$," *Classical Quantum Gravity* **22** (2005), no. 23, 4931–4960.

[45] C. Doran, M. Headrick, C. P. Herzog, J. Kantor, and T. Wiseman, "Numerical Kaehler-Einstein metric on the third del Pezzo," hep-th/0703057.

[46] M. Headrick and A. Nassar, "Energy functionals for Calabi-Yau metrics," 0908.2635.

[47] M. R. Douglas and S. Klevtsov, "Black holes and balanced metrics," 0811.0367.

[48] V. Braun, T. Brelidze, M. R. Douglas, and B. A. Ovrut, "Calabi-Yau Metrics for Quotients and Complete Intersections," arXiv:0712.3563 [hep-th].

[49] V. Braun, T. Brelidze, M. R. Douglas, and B. A. Ovrut, "Eigenvalues and Eigenfunctions of the Scalar Laplace Operator on Calabi-Yau Manifolds," *JHEP* **07** (2008) 120, 0805.3689.

[50] M. R. Douglas, R. L. Karp, S. Lukic, and R. Reinbacher, "Numerical Calabi-Yau metrics," hep-th/0612075.

[51] H. S. C. Okonek, M. Schneider, *Vector Bundles on Complex Projective Spaces*. Birkhauser Verlag, 1988.

[52] L. B. Anderson, Y.-H. He, and A. Lukas, "Heterotic compactification, an algorithmic approach," *JHEP* **07** (2007) 049, hep-th/0702210.

[53] L. B. Anderson, Y.-H. He, and A. Lukas, "Monad Bundles in Heterotic String Compactifications," *JHEP* **07** (2008) 104, 0805.2875.

[54] D. Huybrechts and M. Lehn, "The geometry of the Moduli Spaces of Sheaves," *Aspects of Mathematics* **E 31** (1997).

[55] E. R. Sharpe, "Kaehler cone substructure," *Adv. Theor. Math. Phys.* **2** (1999) 1441–1462, hep-th/9810064.

[56] L. B. Anderson, J. Gray, A. Lukas, and B. Ovrut, "The Edge Of Supersymmetry: Stability Walls in Heterotic Theory," *Phys. Lett.* **B677** (2009) 190–194, 0903.5088.

[57] L. B. Anderson, J. Gray, A. Lukas, and B. Ovrut, "Stability Walls in Heterotic Theories," *JHEP* **09** (2009) 026, 0905.1748.

[58] L. B. Anderson, J. Gray, and B. Ovrut, "Yukawa Textures From Heterotic Stability Walls," 1001.2317.

[59] Y. Sano, "Numerical algorithm for finding balanced metrics," *Osaka J. Math.* **43** (2006), no. 3, 679–688.

[60] M. Headrick and T. Wiseman, "Numerical Ricci-flat metrics on K3," *Class. Quant. Grav.* **22** (2005) 4931–4960, hep-th/0506129.

[61] P. Griffiths and J. Harris, *Principles of algebraic geometry*. Wiley-Interscience [John Wiley & Sons], New York, 1978. Pure and Applied Mathematics.

[62] L. B. Anderson, "Heterotic and M-theory Compactifications for String Phenomenology," 0808.3621.

[63] B. A. Ovrut, T. Pantev, and J. Park, "Small instanton transitions in heterotic M-theory," *JHEP* **05** (2000) 045, hep-th/0001133.

[64] E. Buchbinder, R. Donagi, and B. A. Ovrut, "Vector bundle moduli and small instanton transitions," *JHEP* **06** (2002) 054, hep-th/0202084.

[65] J. Gray, Y.-H. He, and A. Lukas, "Algorithmic algebraic geometry and flux vacua," *JHEP* **09** (2006) 031, hep-th/0606122.

[66] J. Gray, Y.-H. He, A. Ilderton, and A. Lukas, "STRINGVACUA: A Mathematica Package for Studying Vacuum Configurations in String Phenomenology," *Comput. Phys. Commun.* **180** (2009) 107–119, 0801.1508.

[67] G.-M. Greuel, V. Levandovskyy, and H. Schönemann, "Singular::Plural 2.1," A Computer Algebra System for Noncommutative Polynomial Algebras, Centre for Computer Algebra, University of Kaiserslautern, 2003. http://www.singular.uni-kl.de/plural.

[68] D. Kaledin and M. Verbitsky, "Non-Hermitian Yang-Mills connections," *SELECTA MATH.* **4** (1998) 279.

[69] L. B. Anderson, J. Gray, and B. A. Ovrut, "Stability walls and the connected web of heterotic vacua." To appear.

[70] L. B. Anderson, V. Braun, and B. A. Ovrut, "Numerical connections and Kähler cone substructure." To appear.